NASA CONTRACTOR REPORT 177466

An Assessment of Wind Tunnel Test Data on Flexible Thermal Protection Materials and Results of New Fatigue Tests of Threads

C.F. Coe

(NASA-CR-177466) AN ASSESSMENT OF WIND TUNNEL TEST DATA ON FLEXIBLE THERMAL PROTECTION MATERIALS AND RESULTS OF NEW FATIGUE TESTS OF THREADS (Coe Engineering) 70 p CSCL 20A G3/71

N91-13972

Unclas 0320545

CONTRACT NAS2-11420
April 1985

NASA

NASA CONTRACTOR REPORT 177466

An Assessment of Wind Tunnel Test Data on Flexible Thermal Protection Materials and Results of New Fatigue Tests of Threads

C.F. Coe
Coe Engineering, Inc.
Mountain View, CA

Prepared for
Ames Research Center
under Contract NAS2-11420
April 1985

NASA
National Aeronautics and
Space Administration

Ames Research Center
Moffett Field, California 94035

TABLE OF CONTENTS

AN ASSESSMENT OF WIND TUNNEL TEST DATA ON FLEXIBLE THERMAL PROTECTION MATERIALS AND RESULTS OF NEW FATIGUE TESTS OF THREADS

by

Charles Coe
Coe Engineering, Mountain View, CA

ABSTRACT

Advanced Flexible Reusable Surface Insulation (AFRSI) has been developed as a replacement for the low-temperature (white) tiles on the Space Shuttle. The first use of the AFRSI for an Orbiter flight was on the OMS POD of Orbiter .099 for STS-6. Post flight examination after STS-6 showed that damage had occurred to the AFRSI during flight. The failure anomaly between previous wind-tunnel test and STS-6 prompted a series of additional wind-tunnel tests to gain an insight as to the cause of the failure. An assessment of all the past STS-6 wind tunnel tests pointed out the sensitivity of the test results to scaling of dynamic loads due to the difference of boundary layer thickness, and the material properties as a result of exposure to heating.

The thread component of the AFRSI was exposed to fatigue testing using an apparatus that applied pulsating aerodynamic loads on the threads similar to the loads caused by an oscillating shock. Comparison of the mean values of the number-of-cycles to failure showed that the history of the thread was the major factor in its performance. The thread and the wind tunnel data suggests a mechanism of failure for the AFRSI.

AN ASSESSMENT OF WIND TUNNEL TEST DATA ON FLEXIBLE THERMAL PROTECTION MATERIALS AND RESULTS OF NEW FATIGUE TESTS OF THREADS

1 INTRODUCTION

Advanced Flexible Reusable Surface Insulation (AFRSI) has been developed as a replacement for the low-temperature (white) tiles on the Space Shuttle Orbiter. AFRSI is a quilted blanket consisting of silica-fiber insulation as the quilt filler, woven quartz-fiber outer fabric and glass-fiber inner fabric. The quilting is done with quartz thread stitched through the three layers of materials. The quilt cells are nominally 1-inch square and there are approximately four (4) quilt stitches per inch. The thickness of the quartz fabric is 0.027 inch and the diameter of the quilting thread is about 0.02 inch.

There are four potential causes of AFRSI failure. They are:

1. IMPACT
2. ABRASION BY PARTICULATES
3. STATIC STRENGTH LIMITS EXCEEDED
4. FATIGUE

Causes 1 and 2 relate to foreign-object damage. Causes 3 and 4 potentially result from aerodynamic loads during Orbiter launch and entry atmospheric flight. Loads on the AFRSI occur due to pressure differences through the fabric and drag (skin friction). Because the AFRSI is porous, maximum normal loads occur where pressure gradients and fluctuating pressures are high, such as in the regions of shock waves and separated flow. As with all porous media, the amplitude and phase angle of propagating fluctuating pressures vary with frequency such that higher frequency pressures will result in higher loads. Material properties as a function temperature are a critical factor relative to AFRSI failure. With respect to fatigue, the fibers in the threads can be subject to self abrasion and thus the length of time under load along in conjunction with the amplitude and frequency is critical.

The first application of AFRSI for an Orbiter flight was on the OMS pods for STS-6. Examination of the AFRSI during orbit of STS-6 showed that no percepible damage had occurred due to the launch environment; however, post flight inspection showed that damaged had occurred during entry. The anomaly between previous wind-tunnel tests and STS-6 prompted a series of additional wind-tunnel tests to gain insight into the causes of the problem and to evaluate possible fixes. The wind-tunnel tests of interest were designated OS-314, OS-315, OS-316 and OS-318 (Refs. 1 to 6). OS-314 and previous wind-tunnel certification tests were conducted in Ames Research Center (ARC) Unitary Plan wind tunnels at ambient temperatures. OS-315, OS-316 and OS-318 test were conducted at Arnold Engineering Development Center (AEDC) in the Aerothermal Tunnel C at both ambient and approximately 1300°F total temperatures. The flow simulation during certification tests included high pressure gradients and fluctuating pressures that occur in regions of shock waves and separated boundary layers.

Originally, ambient-temperature certification tests of AFRSI were considered adequate because static-strength tests of the quartz fabric did not degrade the strength of the material sufficiently to negate the validity of ambient-temperature tests. The fact, however, that AFRSI damage occurred on STS-6 during entry showed that the certification tests had not been adequate. It was rationalized that some aspect of the flow simulation, such as votex impingement, had not been covered, or probably that temperature effects were greater than expected. Tests OS-315 and OS-318 did in fact show temperature effects on times to failure of AFRSI. Tests OS-314 (ARC) and OS-315 (ARDC), however, also showed differences in times to failure at ambient temperature conditions.

Because of the above mentioned anomalies between the ARC and AEDC tests, this contract was initiated to assess the post STS-6 wind-tunnel data and to conduct some simple new baboratory tests to investigate the fatigue characteristics of AFRSI thread.

The contract was sponsored by NASA Ames Research Center; the technical monitor was Mr. S. R. Riccitiello. The author wishes to acknowledge the support of Mr. J. J. Barneburg of NASA Lyndon B. Johnson Space Center (JSC) and Mr. P. L. Lemoine of Rockwell International Corporation (RI).

2 NOTATION

a	double ampliitude
CP	pressure coefficient
f	frequency
G(f)	power spectral density
IR	infrared
M	Mach number
N	number of cycles to failure
OASPL	overall sound pressure level
P	static pressure
P_{REF}	static pressure at reference orifice in thread fatigue test fixture
Prms	root-mean-square of pressure fluctuation
PT	total pressure
ΔP	pressure rise across shock wave
q	freestream dynamic pressure
RE	Reynolds number
RPS	revolutions per second
SPL	sound pressure level
t	time
TC	thermocouple
TSmax	maximum AFRSI static temperature
TT	total temperature
U	freestream velocity
V	velocity
X	longitudinal distance from leading edge of test fixture
Y	lateral distance from centerline of fixture
Z	distance normal to surface of test fixture
α	angle-of-attack
δ	boundary layer thickness

3 SCALING OF FLUCTUATING PRESSURES

An important issue relative to wind-tunnel tests of AFRSI is that it was necessary to test full-scale articles. As a consequence, many of the tests were conducted in ARC wind tunnels that allowed large test fixtures that could yield boundary-layer conditions similar to those expected on the Orbiter. Environmental temperatures in the ARC wind tunnels, however, were limited to ambient temperatures. After STS-6 other tests were conducted at AEDC where temperatures could be varied to simulate entry temperatures. For the AEDC tests boundary layers probably were subscale.

To illustrate the relationship of the boundary layer to the scaling of pressure fluctuations in regions of shock waves and supersonic attached and separated flows, Figures 1 and 2 are taken from Ref. 6. Figures 1 and 2 show that the mean-square amplitudes of fluctuating pressures are inversely proportional to the boundary-layer thickness and that the frequencies are directly proportional to the boundary-layer thickness. When, for example, the pressure differences across shock waves and the freestream dynamic pressures are the same for different boundary layer thicknesses, the integrated pressure fluctuations or OASPL's are unchanged. Thus the surface pressure fluctuations caused by thick boundary layers occur in a lower frequency band than those caused by thin boundary layers.

Another affect of boundary-layer thickness is that the amplitudes of the shock-wave motion and corresponding flow-separation and attachment boundaries are proportional to the boundary-layer thickness. Figure 3 illustrates this effect on AFRSI. If for two test cases (A and B) the pressure-rise through the shock waves are duplicated, than Prms and OASPL (db) will be the same in both cases. The fluctuating pressures will be spread over more AFRSI cells and the frequency band will be lower for Case A than for Case B because the boundary layer is thicker for Case A. Conversely the fluctuating pressues for Case B will be confined to fewer AFRSI cells and the frequencies will be higher than for Case A.

A hypothesis of an AFRSI failure and the effects of boundary-layer thickness is suggested in Figure 4. The basis of the argument is that the quartz fabric is initially taught due to the quilting through the filler material. The filler material has very low resiliency and consequently it compresses further without rebounding with each cycle of applied load. The amplitudes of the fabric and also the quilting thread will thus increase with each oscillation. As the amplitudes increase the curvature of the cloth increases to the point of filament fractures and/or the deterioration of fibers increases due to self abrasion. The effects of a thinner boundary layer at conditions of constant temperature, ΔP across the shock wave and OASPL would be to reduce the time for the fabric oscillations to increase in amplitude. For equal conditions a thinner boundary layer would therefore result in lower time to failure of AFRSI.

4 ASSESSMENT OF POST STS-6 WIND TUNNEL TESTS

4.1 OS-314

Test OS-314 (Ref. 1) was conducted in the ARC 9-x 7-Foot Supersonic Wind Tunnel (9x7 SWT) as the first of a series of tests (OS-314, OS-315, OS-316, OS-318) to help resolve an anomoly between previous proof and certification tests and the flight damage of AFRSI during STS-6. The test apparatus was a previous test fixture which was modified to closely simulate pressure-gradient loads and OASPL's at the forward end of the OMS pods. A vortex generator was also employed to evaluate the effects of shed vortices striking the AFRSI. Figures 5 and 6, taken from Ref. 1, show the general arrangement and installation of the test fixture in the ceiling of the 9x7 SWT. The boundary-layer thickness at the flow separation point was about 4.5 inches.

Several AFRSI panels were tested during OS-314. Some were preconditioned for the ascent simulation, some were thermally conditioned at 1100°F for entry simulation, and some alternate designs were also tested. Two panels that were tested were taken from Orbiter Vehicle OV-099 after the STS-6 mission. Complete details of the tests and results are given in Ref. 1. From three baseline AFRSI panels tested at ascent conditions the results show that one panel was damaged after 200 seconds with q=400 psf, the second panel was damaged after 325 seconds with q=550 psf, and the third panel was damaged at q=560 psf (time not specified). The maximum dynamic pressure (q) of the ascent simulations for baseline AFRSI varied from 523 psf to 629 psf. Three entry simulations of 250-second duration each were conducted with the same AFRSI test article which had been thermally preconditioned at 1100°F. No damage was observed. Two additional entry simulations of 250-second duration each were conducted with the AFRSI removed from OV-099, and no damage was observed. The maximum q for the entry conditions was 160 psf, and the maximum OASPL was about 153 dB near the leading edge of the AFRSI.

The dichotomy of the OS-314 tests relative to STS-6 is that OS-314 showed AFRSI failures at dynamic pressures less than the ascent dynamic pressure for STS-6. OS-314 also showed no failures for entry conditions when in fact AFRSI was damaged during entry of STS-6. Examination of fixture calibration data showed that ascent and entry steady and fluctuating-pressure loadings were simulated as well as can be expected. There were two critical shortcomings of the OS-314 simulation, however. One shortcoming was that the tunnel drive time required to arrive at test conditions was long, which compromised the load simulations of dynamic pressure versus time. Consequently, the failures of the AFRSI during the ascent simulation can probably be attributed to the mismatch of the profiles of dynamic pressure versus time. The other shortcoming of the OS-314 simulation was the inability to simulate entry temperatures. It is not clear, however, that entry temperatures must be duplicated during the test. Aside from the possible affects of temperature on Reynolds number and flow separation it would not be expected that the environmental temperature would effect the performance of AFRSI that has been preconditioned by exposure to entry temperatures. For OS-314 one test article had been thermally preconditioned at 1100°F and one test article had been taken from OV-099 after STS-6. Why then was there no damage of these test articles? One possibility is that the residual amount of teflon, which coats the quartz fibers in the AFRSI as received from the manufacturer, had not been duplicated during OS-314 and STS-6. Also it is possible that the number of samples tested may have been insufficient to obtain an adequate statistical accuracy.

To illustrate the effects of residual teflon, Figure 7 shows Thermo Gravimetric Analyses (TGA) of AFRSI threads. The TGAs show the percent of orginal weight of an AFRSI thread speciman versus temperature. The weight loss that occurs with increasing temperature is due to the vaporation of the teflon. These TGAs therefore show that a temperatuue of at least 1100°F was required to vaporize all the teflon. As previously mentioned one of the OS-314 test articles was thermally preconditioned at 1100°F, and while the precise thermal exposure of the OV-099 test article is not known it is believed that it was less than 1100°F. New tests of AFRSI threads, which were conducted as part of this investigation and are described in a later section of this report, show that the teflon content in the AFRSI threads has an extremetly large effect on the thread fatigue properties.

4.2 OS-315

Test OS-315 was conducted at AEDC in the Mach 4 Aero Thermal Wind Tunnel C (Ref.2). The objective of OS-315 was to assess the survivability of AFRSI under the influence of similar air loads specified for OS-314 plus entry surface temperatures. A sketch of the test fixture used for OS-315 is shown in Figure 8. The fixture is an AEDC facility wedge that was modified to add a two-dimensional AFRSI test region that simulated the shape and pressure distribution on the foward part of the OMS pod. In contrast to the tunnel ceiling mounting of OS-314, this fixture is injected into the wind-tunnel freestream flow. A decided advantage of this procedure is that tunnel start-up and shut-down times are of no concern. The duration of test article expossure to the preset environment could therefore be precisely controlled and failure times could be accounted to a known set of constant conditions. A possible disadvantage of the AEDC fixture is a subscale boundary layer on the AFRSI.

Table 1 (Table 2 in Ref. 1) shows the tunnel and test article parameters for OS-315. Three AFRSI articles were tested: (1) sample A which was baseline AFRSI, (2) sample B which was baseline AFRSI which had been thermally preconditioned at 1100°F and (3) sample F which had been removed from OV-099 after STS-6.

Sample A was tested twice at ascent conditions. The first test with ΔP=0.81 psi and OASPL=158 dB showed no signs of failure after 252 seconds. The second test of Sample A with ΔP=1.2 psi and OASPL=160.4 dB failed after 102 seconds with an accumulative total time of 354 seconds. For comparison the closest ascent test conditions for OS-314 had a ΔP=1.65 psi and OASPL=164.9 dB. At these OS-314 conditions the AFRSI showed signs of damage at 200 seconds. If allownaces are made for the differences in environmental loads for OS-314 and OS-315, the times-to-failure observed from the separate wind-tunnel tests are comparable.

One of the important differences between the OS-314 and OS-315 environments is the boundary-layer thickness and its affect on the frequency spectra of the fluctuating pressures. Figures 9 and 10 illustrate 1/3-octave spectra for OS-314 and OS-315 for OASPLs of 158 dB and 160.4 dB respectively which were the acoustic levels of the two AFRSI OS-315 Sample A tests. The OS-314 spectra were scaled to the OS-315 OASPLs taking into account the different boundary-layer thicknesses. (The boundary-layer thicknesses at the shock waves on OS-314 and OS-315 were approximately 4.5 and 0.7 inches respectively. The OS-315 boundary layer thickness was based on measurements obtained during OS-318). As can be seen from Figures 9 and 10 the thinner boundary layer of OS-315 shifts the pressure fluctuations to higher frequencies. Thus more cycles of fiber bending occurred per second for OS-315 samples than for OS-314 samples.

Samples B and F were tested at entry conditions with ΔP=0.76 psi and OASPL=158 dB (Table 1). Surface temperatures during the tests varied from 925°F to 990°F on Sample B and from 820°F to 850°F on Sample F. Under these conditions Sample B failed after 52 seconds and Sample F failed after 44 seconds. The thermally preconditioned and OV-099 AFRSI samples tested in OS-314 did not fail. These differences in AFRSI performance could only have been due to differences in loads, including the effect of dynamic scaling, and/or the effects of the different environmental temperatures.

As previously mentioned, the earlier ARC tests had been justified by the belief that baseline AFRSI performance would not be affected by the environmental temperature (for constant load conditions) provided the material had been thermally preconditioned at the maximum expected entry temperature. For this reason, the aerodynamic data have been examined to determine if there was some characteristic relating to the loads that could account for the differences in failure times from the ARC and AEDC tests. The results of the examination of data suggest that the OS-315 AFRSI failures were premature because the loads in the regions of initial failures were higher than expected.

Figures 11 and 12 show the static-pressure and fluctuating-pressure distributions on the OS-315 fixture when the tunnel total temperature (TT) was 340°F. Reynolds-number per foot was 1.39 million. The leading edge of the AFRSI was at X=15.5 inches. Therefore the data of interest are the longitudinal and lateral pressures where the separated boundary layer became reattached. Figures 11 and 12 show that there was relatively little lateral variation in the presures at TT=340°F. Figures 13 and 14 show the same pressure distributions when the tunnel was set for entry simulation with TT=1436°F. Reynolds-number per foot was 0.38 million. These data now show that there were large differences in the lateral pressures at entry conditions. The OASPL, for example, was 6 dB higher (factor of 2) at Y=3.86 inches then at the centerline. If the maximum off-centerline OASPL can be taken to be the centerline maximum OASPL plus 6 dB, then the OASPL on the AFRSI samples tested for entry conditions would have been higher than the OASPL for the ascent tests (164 DB versus 160.4 dB). The maximum OASPL for the entry conditions for OS-314 was 153 dB and there was no AFRSI damage. Because of the large differences in the maximum OASPLs for entry simulations during the OS-314 test (153 dB) and OS-315 test (possibly as high as 164 dB) it is not possible to conclude whether the entry temperature environment during the OS-315 test significantly altered the material properties of the thermally preconditioned test samples.

Figures 15 and 16 show post test photographs of Samples B and F. As can be seen, the damage was extensive on both samples. Test notes recorded that the damage commences off centerline, which correlates with the higher off-centerline loads. For comparison purposes, figure 17 shows a post test photograph of the Baseline Sample A which was tested at ascent conditions. In this case the AFRSI damage started nearer to the centerline. It is interesting that a similar damage pattern can be seen near the centerline in the post test photograph for Sample B (Fig. 15).

4.3 OS-316

Test OS-316 (Ref. 3) was conducted in the AEDC Aerothermal Wind Tunnel C to determine the survivability of AFRSI under aerodynamic and thermal conditions that sumulated the rudder/speed brake area of the Orbiter during entry. The same test fixture used for the OS-315 test was used for the OS-316 test.

There were four AFRSI samples tested. One sample was the baseline configuration that had been thermally preconditioned at 1200°F and not rewaterproffed. The other three samples were baseline AFRSI that had been coated wih C-9 ceramic, thermally preconditioned and not rewaterproofed. Test OS-316 clearly demonstrated a significant improvement in AFRSI survivability due to the ceramic coating. The one uncoated sample failed after 27 seconds of exposure to an OASPL of 162 dB and tunnel total temperature of 1435°F. The coated samples survived one hour of cumulative exposure to the same test conditions.

4.4 OS-318

Test Os-318 was the most comprehensive post STS-6 wind-tunnel test of AFRSI (Ref. 4). It was conducted in the AEDC Aerothermal Wind Tunnel C to (1) re-establish the operational limits of AFRSI and (2) to investigate the effects of deviations in fabrication and installation, the effectiveness of repairs, and possible improvements in survivability afforded by external coatings. A total of 63 samples were tested at a Mach number of 3.92 with total pressures from 25 to 80 psia and total temperatures from 300°F to 1440°F.

The test fixture for OS-318 included the AEDC wedge fixture that had been modified to accommodate flat AFRSI samples. The fixture also incorporated a flap near the trailing edge and provisions for installation of a wedge assembly. The flap could be raised or the wedge installed to generate the desired shock waves and corresponding ΔPs and OASPLs over the samples. Figures 18 and 19 (taken from Ref. 4) show the test fixture and shock generator assembly.

Of the 62 samples tested during OS-318, only the tests of the baseline AFRSI are relevant to this assessment. Table 2, which includes parts of Table VII from Ref. 4, shows the run schedule and pertinent test conditions for the runs of interest. A column that shows the AFRSI static temperatures measured by infrared sensing and thermocouple instrumentation has been added to the table. The static-temperature data show that for entry conditions infrared sensed temperatures varied from 810°F to 1120°F and thermocouple sensed temperatures varied from 870°F to 1400°F. Only two of the samples tested at entry conditions were thermally preconditioned (at 1200°F). Therefore, for many entry runs, depending upon the actual material temperatures, some teflon may have still been present in the AFRSI threads. Refer to Figure 7 for examples of TGSs of AFRSI threads.

Figure 20 shows time-to-failure of AFRSI baseline samples tested during OS-318. The data show that at ascent temperatures AFRSI failure times varied from over 30-minutes when the OASPL was 161.5 dB to near zero-minutes when the OASPL was 166 dB. When temperatures were at enty conditions the data show extremes of less than one-minute to failure at an OASPL of 155 dB to 55-minutes at an OASPL of 162.2 dB. The trend of time-to-failure versus load at entry temperature is unclear, however, it is evident that the average failure time was less than for ascent temperatures.

Because of the lateral variation of aerodynamic loads that occurred on the OS-315 fixture due to tunnel temperature, Os-318 data were examined for possible similar characteristics. Static-pressure distributions and boundary-layer profiles are therefore shown in Figures 21 and 22 for ambient and entry total temperatures. These data show that the flow was more two-dimensional for OS-318 than for OS-315. The pressure coeficients at Y= -3.25 inches and Y=5.25 inches were less than at the centerline, however, the pressure rises across the shock wave at the flow attachment point were not significantly affected. These data show that tunnel temperatures had no detrimental effect on the AFRSI loads during OS-318.

4.5 CONCLUDING REMARKS ON THE ASSESSMENT OF POST STS-6 WIND TUNNEL TESTS

At the outset of this investigation there was concern at ARC for the differences in the AFRSI damage experience from Orbiter flight STS-6 and from post STS-6 wind-tunnel tests at ARC and AEDC. The fact that AFRSI damage occurred on STS-6 but did no occur during ARC test OS-314 with entry load simulation on thermally preconditioned panels pointed to the possible requirement that the test environments included entry temperatures. AFRSI was damaged when entry temperatues were included during AEDC tests OS-315, OS-316 and OS-318.

This assessment has pointed out the sensitivity of the test results to dynamic scaling of dynamic loads due to differences in boundary-layer thickness. It has also pointed out the possibility that material properties may have varied due to different amounts of teflon remaining on the AFRSI threads during the entry tests. In addition it was revealed that the maximum entry loads were higher for the AEDC tests than for the ARC test. Therefore, direct comparisons of AFRSI preformance from these test cannot be used to resolve whether tests of thermally preconditioned panels at ambient temperatues are equivalent to tests conducted at entry temperatures.

There is no doubt from the post STS-6 test results that AFRSI performance is more sensitive to entry temperature exposure than projected from static strength tests. Some other aspect of the material properties that would be strongly affected by the amount of teflon in the thread, such as fatigue due to self abraision, must therefore be critical.

5. FATIGUE TEST OF AFRSI THREADS

5.1 INTRODUCTION

As a consequence of the foregoing assessment of AFRSI performance during post STS-6 wind-tunnel tests a simple laboratory test was conducted to investigate the fatigue characteristis of AFRSI threads exposed to dynamic loads. The effects of the amount of teflon on the threads is of interest because the teflon content will vary from the first ascent to entry, depending upon entry temperatures, and thence to succeeding ascents and entry cycles.

As previously discussed loads on the AFRSI occur due to pressure differences through the fabric that cause lift and drag, including skin friction. The quilt stitching threads can experience highly pulsating drag loads due to the alternating separation and attachment of the boundary layer where shock waves occur. An illustration of the source of the pulsating drag loads is shown in Figure 23. The figure also illustrates the affect of boundary-layer thickness on the amplitude of the pulsations. The velocity profiles in Figure 23 were measured on the wall of the ARC 9x7 SWT during the tests reported in Ref. 7. The different ΔVs that are shown for OS-314 and OS-318 would occur at approximately 0.03-inch above the AFRSI surface, which is possible for the AFRSI quilting threads. The pulsating drag loads resulting from the ΔVs would be proportional to ΔV^2.

This fatigue test of AFRSI threads was conducted by exposing the threads to pulsating loads from an air jet. The effects of the standard AFRSI heat cleaning cycle (650°F for 4 hours followed by 850°F for 2 hours) and thermal preconditioning at 1200°F for 10 minutes were investigated. In addition, the effects of the number of entry cycles and the thread clearance above the surface were also investigated.

5.2 TEST APPARATUS

A sketch of the test apparatus used for the AFRSI thread fatigue test is shown in Figure 24. The apparatus provided the means of inducing pulsating loads on the threads by rotating a thread speciman mounted on a shaft in a continuous flow air jet. The shaft spanned a channel that contained the air flow. The thread span on the shaft was 1/4 inch and the nominal clearance under the thread was 0.031 inch. The thread passed through holes in the shaft that had been slightly chamfered and polished at the hole openings to minimize abrasion. All thread specimens were bonded to the face of the shaft opposite the loop while fixed dead-weight loads hung from the loose thread ends. Generally, to facilitate the testing, thread samples were bonded into several shafts at one time. The installed shaft with thread was rotated on an electric motor capable of speeds in excess of 300 revolutions-per-second (RPS). The shaft RPS was monitored by a photo detector and counter and the flow conditions were monitored by a reference static-pressure orifice. Dynamic pressure transducers were also installed in one wall of the channel to determine the OASPLs downstream of the shaft. Photographs and engineering drawings of the apparatus are shown in Figures 25 and 26.

5.3 CALIBRATIONS

Originally it was not considered necessary to calibrate the air flow in the channel. It was at first assumed that any arbitrary air flow could be established by the reference pressure and then repeated for each AFRSI thread tested. The only sought after results were the lengths-of-time to failure of the threads at a constant applied force by the jet. (Centrifugal-force effects were neglected). Unfortunately it was found that one jet-flow setting was not suitable for all thread conditions and it therefore became necessary to calibrate the channel. The shaft was removed for the calibrations. The calibrations, which are shown in Figure 27, in terms of dynamic pressuue versus reference static pressure were determined from measurements of wall static pressure and air-flow total pressure at the shaft centerline. The data show that the range of dynamic pressures for the thread test was from about 200 psf to 4,200 psf.

As previously mentioned the fluctuating pressures were measured at three locations on the channel wall downstream of the shaft. Two locations were respectively at 1-inch and 1.5-inches downstream of the shaft centerline and one location was 1-inch downstream and 1/4-inch above the shaft centerline.

The measurements were not an essential part of the investigation, but the fluctuating pressures and OASPLs are of interest relative to other AFRSI investigations. The measurements in terms of Prms and OASPL are shown in Figures 28-30 and are tabulated in Table 3. The frequency band-width represented by data was from about 1 Hz to 5,000 Hz. The data show that the pressure fluctations varied from about 0.035 psi rms at the lowest reference pressure setting of 0.02 psi to about 0.68 psi rms at the highest reference pressure of 0.8 psi. The effects of the shaft RPS were small. The discontinuity at a reference pressure of 0.8 psi was due to screeching of the jet at this pressure. The OASPLs of the pressure fluctuations varied from about 142 dB to 167 dB for the range of reference pressure settings.

5.4 THREAD CONDITIONS TESTED

There were three basic thread conditions tested. For the baseline condition the threads tested were thermally preconditioned at atmospheric pressure at the so-called "heat-cleaned" condition for 4 hours at 650°F plus 2 hours at 850°F. The main variation of the baseline condition was the entry condition for which heat-cleaned threads were further thermally preconditioned at atmospheric pressue for 10 minutes at 1200°F. (Some thread samples were preconditioned for entry in a vacuum and tested to show that preconditioning in a vacuum environment was unnecessary). The third basic thread condition tested was "off spool" as received from the manufacturer. A variation of the entry condition was to repeat the entry preconditioning in order to investigate the effect of the number of entry cycles.

The effects of the thermal preconditioning were found to be crucially important with respect to the thread fatigue properties. The off-spool thread contains about 18-percent teflon by weight, ± 2 percent, and the amount of teflon is affected by the thermal preconditioning; thus the fatigue properties of the thread are affected. This affect is illustrated by the TGAs shown in Figure 7, which were described in paragraph 4.1. The TGAs show that nearly all the teflon is vaporized from the threads at temperatures between 500°C and 600°C (932°F and 1,112°F). Because this temperature range is higher then the heat-clean temperatures, there was very little difference between the

TGAs for the off-spool thread (Fig. 7a) versus heat-cleaned thread (Fig.7b). The data show about 1-percent less weight loss from the entry-cleaned thread than from the off-spool thread. This difference is within the accuracy specifications of the analysis; however, if correct, it still shows that 95-percent of the teflon remains on the thread after heat cleaning.

5.5 TEST PROCEDURE

A total of about 175 thread samples were tested in order to evaluate the number of cycles-to-failure of the AFRSI threads. The number of samples tested varied with each thread condition depending upon the scatter of the data. Tests were conducted at reference pressures from .02 psi to 0.8 psi with shaft speeds at 50 to 300 RPS. The specific test conditions for the different threads were selected by trial so that thread failure times were greater than zero and less than 1,800 seconds. Tests were stopped at 1,800 seconds.

A test procedure was followed that minimized the effects of start-up load cycles. First, the desired speed of the shaft drive motor was preset with a vernier control using a shaft without thread. A test shaft with thread was then installed and hand rotated to position the thread on the leeward side of the shaft. The air flow was adjusted to give the desired reference pressure and a switch was closed to start the motor. Shaft speed and constant cyclic loads were attained within a few load cycles. The time-to-failure of the thread in seconds was recorded.

Additional tests were conducted to obtain a photographic record of the progression of AFRSI thread failures for heat-cleaned and entry threads. For these tests the shaft with thread was removed after various test intervals, then photographed and reinstalled to continue the progression to the time of thread failure.

5.6 RESULTS AND DISCUSSION

5.6.1 Loop Clearances of 0.031 Inch

The results of all the thread tests with loop clearances of 0.031 inch are tabulated in Table 4. The tables show thread-failure times for the various reference-pressure and shaft-RPS settings for each of the thread conditions tested. The thread conditions were "heat cleaned" (650°F for 4 hours plus 850°F for 2 hours), "entry" (heat cleaned plus 1,200°F for 10 minutes) and "off spool". The tabulations also show the number of tests at each load condition, the maximum and minimum reading, the mean of the recorded failure times, the mean of the number of load cycles to failure and the corresponding standard deviations.

The first important result revealed by the tabulations are the vary large variations in recorded times to failure of all threads when at any constant load condition. The differences in minimum and maximum failure times were generally at least a factor of 10. Such results indicate that certification tests of full-scale uncoated AFRSI using only a few samples would have questionable reliability. The tabulated results also show the extremely large range of load conditions that was required to obtain useful data. No egual-load condition could be applied to more than one of the three thread conditions. This result was not surprising, but it was inconvient because it made it necessary to measure the relative applied loads and then to base comparisons of the thread fatigue life on extrapolated data.

Plots of the mean values of the number of cycles-to-failure are shown versus reference pressure in Figure 31 and versus normalized force in Figure 32. The plotted mean values are those from Table 4 that were relatively unaffected by 0 or 1,800-second thread failure times. The normalized forces were assumed to be proportional to the dynamic pressures at the shaft centerline (Fig. 27). The data show that, no matter how the results are presented and extrapolated to equal load conditions, there were extremely large differences in the number of cycles-to-failure for the different thread conditions. It appears that the number of cycles-to-failure for threads preconditioned at/or exposed to 1,200°F entry temperatures would be less than one-millionth the number of cycles for heat cleaned threads at ascent condition. The data also show that the heat cleaned threads would fail at less than one-tenth the number of cycles for off-spool threads. Such results show that the fatigue properties of the AFRSI are so strongly affected by preconditioning temperatures that it would be almost impossible to depend on qualification test data for high temperature applications unless the preconditioning or tests were conducted at temperatures above 1,100°F (see TGAs in Fig. 7). Unfortunately, the fatigue life of the material or dynamic strength appears to be almost zero. These results confirm the need for the ceramic coating that has now been applied to AFRSI on Orbier vehicles.

There is little doubt that the large differences in fatigue life of the AFRSI threads for different thermal preconditioning were due to the effects of the amount of teflon in the thread. Figure 3 illustrates this point by showing photographs of the progressive failure of heat-cleaned threads (Fig. 33a) and entry preconditioned threads (Fig. 33b). Note that the reference pressures were 0.5 psi for the heat-cleaned thread and 0.02 psi for the entry thread. The photographs show that the thread with teflon behaved as a composite material and that failure commenced within a few load cycles from total loss of the thread. Recall from Figure 7 that nearly 20-percent of the thread weight in the heat-clean condition is teflon. The entry preconditioned thread, on the other hand, with the teflon completely vaporized from the thread failed by progessive fracture and unraveling of the quartz filaments.

5.6.2 Effect of Loop Clearance

As previously mentioned in paragraph 5.2 the baseline loop-clearance of 0.31 inch was selected in order to obtain failures of off-spool threads at the upper limit of reference pressure. Tests of entry preconditioned threads were therefore conducted to determine the effects of changing the loop clearance. The results (Fig. 34) show that loop clearances less then 0.031 inch had very little effect on the number of cycles to failure for entry-conditioned threads, whereas, loop clearances greater than 0.031 inch caused a substantial reduction in the number of cycles to failure.

5.6.3 Effect of Number of Entry Preconditioning Cycles

It would hardly be expected that the fatigue characteristiis of the AFRSI threads would be affected by repeated entry heat cycles if all the teflon was vaporized during the first heating cycle. Nevertheless, additional tests were conducted to evaluate the effect of the number of entry preconditioning cycles. As part of these tests some thread samples were thermally preconditioned and cooled in a vacuum and tested within 45-minutes after cooling to room temperature and some samples were thermally preconditioned and cooled at atmospheric pressure and tested after 24 hours. The reason for the vacuum and air preconditioning was to confirm that the use of thermal preconditioning at atmospheric pressure for all the other threads tested was acceptable. The results of these tests, which were conducted at a reference pressure of 0.04 psi, are shown in Figure 35.

The data in Figuue 35 show trends of slight reductions in number-of-cycles to failure of AFRSI threads for increasing numbers of entry preconditioning cycles for both the vacuum and air thermally preconditioned threads. These trends, however, and the effects of vacuum versus air thermal preconditioning are insignificant relative to the scatter of data samples.

5.7 CONCLUDING REMARKS ON FATIGUE TESTS OF AFRSI THREADS

Fatigue tests of AFRSI threads were conducted using an apparatus that applied pulsating aerodynamic loads on the threads similar to the loads caused by oscillating shock waves. Three threads conditions were tested: (1) Threads were thermally preconditioned (heat cleaned) to simulate the ascent condition at 650°F for 4 hours plus 850°F for 2 hours; (2) Heat cleaned threads were further thermally preconditioned to simulate the entry condition at 1,200°F for 10 minutes; (3) Threads were taken "off spool" as delivered. The tests were conducted over a range of dynamic pressures from about 200 psf to 4,200 psf.

The thread fatigue tests showed a large scatter in data samples. For a constant test condition the ratio of maximum-to-minimum number of load cycles to failure was about 10. Comparison of the mean values of the number-of-cycles to failure showed that there was an extremely large reduction, greater than a factor of one million, in the fatigue life of the threads that had been thermally preconditoned at 1,200°F. There is little doubt that this large reduction in fatigue life was due to the elimination of teflon in the thread by the entry thermal preconditioning. The results of the test suggest that, if there is no teflon or other precoating on AFRSI thread, the material may not be suitable for aerodynamic applications unless the dynamic environment is benign.

6 REFERENCES

1. SAS/AERO/84-304, "Space Shuttle AFRSI OMS Pod Environment Test using Model 81-0 Test Fixture in the Ames Research Center 9 x7-Foot Supersonic Wind Tunnel (OS-314A/B/C), "Rockwell International Corporation April 1984.

2. IL 712-83-ECK-054, "Summary Data Report from OS-315 AFRSI Combined Environments Test", Rockwell International Corporation, Octoer 1983.

3. IL 712-83-ECK-057, "Appendix Containing Data Results from OS-315 AFRSI Combined Environments Test", Rockwell International Corporation, October 1983.

4. SAS/AERO/84-321, "Results of the Space Shuttle Orbiter Speed Brake AFRSI Integrated Environments Tests OS-316 in the AEDC VKF Tunnel C", Rockwell International Corporation, June 1984.

5. SAS/AERO/84-312, "Results of the Space Shuttle Orbiter AFRSI Integrated Environments Tests 318 in the AEDC VKF Tunnel C", Rockwell International Corporation, May 1984.

6. Final Data Package from Arnold Engineering Development Center for Project Number CB42VC (V--C-3K) covering tests Entitled "SD/NADA AFRSI Characterization" (OS-318). Tests conducted in Aerothermal Tunnel C January through March, 1984.

7. Coe, C. F., Chyu, W. J., and Dods, Jr., J. B.: Pressure Fluctuations Underlying Attached and Separated Supersonic Turbulent Boundary Layer and Shock Waves, AIAA Paper No. 73-996, October 1973.

TABLE 1

TUNNEL AND TEST ARTICLE PARAMETERS

TUNNEL PARAMETERS

CAL RUN	RUN NO.	SAMPLE	TOTAL PRESSURE	TOTAL TEMPERATURE	DYNAMIC PRESSURE	RE/FT
12	23	A (Baseline)	19.9 psi	180→204°F	224 psf	1.48×10^6
9	24	A (Baseline)	25.0	313	282	1.39×10^6
19	29	B (Baseline (1100°F Thermal Cond.)	20.0	1115	221	3.80×10^5
19	30	F (STS-6 Blanket)	20.2	978	224	4.41×10^5

SAMPLE HISTORY

CAL RUN	RUN NO.	SAMPLE	EXPOSURE TIME TO FAIL	TOTAL EXPOSURE TIME	SURFACE TEMP. AT FAILURE	ΔP	ACOUSTIC LEVEL
12	23	A	No Failure	252 sec	Approx. 140°F**	.81 psi	158 db
9	24	A	102 sec	252	Approx. 230°F	1.20	160.4
19	29	B	52	97	925-990°F	.76	158
19	30	F	44*	109	820-850°F	.76	158

*Small breach in facecloth on left side; damage started expanding at 52 sec; damage on right side started at 55 sec.

**Estimated maximum surface temperature at end of exposure.

ORIGINAL PAGE IS
OF POOR QUALITY

TABLE 2

REF. 4 - TABLE VII RUN SCHEDULE (Continued)

RUN	PT PSIA	TT DEG F	RE FT-1	Q PSF	V FT/SEC	SHOCK GENERATOR ANGLE DEG	SHOCK GENERATOR X,IN	SHOCK GENERATOR Y,IN	WEDGE DEG	S.L. THEOR	FLAP	SAMPLE	TIME	TS_{MAX}, ^{o}F IR - TC
51	64.1	301.0	1.43E+06	674.7	2031.				0.00	0.386	60.00			
52	59.6	303.0	1.09E+06	663.9	3333.				0.06	0.400	60.00			
53	49.9	305.0	2.67E+06	566.1	2630.	30.0	21.00	7.50	0.06	0.360				
54	64.1	304.0	1.43E+06	674.6	2633.	17.0	10.00	7.50	0.02	0.385				
55	64.0	355.0	1.60E+06	668.7	3345.	10.0	10.00	7.50	0.01	0.400				
56	49.6	762.0	1.36E+06	551.3	3355.	30.0	21.00	7.50	0.06	0.426				
57	50.1	319.0	1.18E+06	557.7	3507.	30.0	21.00	7.50	0.05	0.440				
58	64.1	310.0	1.41E+06	665.3	3502.	10.0	10.00	7.50	0.09	0.424				
61	59.9	1103.0	1.16E+06	655.0	3836.	10.0	10.00	7.50	0.08	0.442				
62	50.1	1104.0	9.59E+05	540.0	3830.	30.0	21.00	7.50	0.00	0.450				
63	6.1	1107.0	8.37E+04	47.0	3814.	30.0	21.00	7.50	5.05	0.740				
64	59.3	1101.0	9.87E+05	551.4	3822.	30.0	21.00	7.50	-6.01	0.458				
65	49.9	1203.0	4.67E+05	543.7	3951.	30.0	21.00	7.50	0.05	0.467				
66	49.7	1136.0	7.80E+05	512.0	4746.	30.0	21.00	7.50	0.06	0.407				
67	79.9	1181.0	5.76E+05	370.9	3817.	30.0	21.00	7.50	0.05	0.500				
68	60.5	1180.0	1.16E+06	662.2	3810.	30.0	21.00	7.50	0.06	0.441				
69	70.3	1186.0	1.38E+06	760.0	3823.	30.0	21.00	7.50	0.00	0.420				
70	70.0	1098.0	1.59E+06	760.1	3776.	30.0	21.00	7.50	0.04	0.426				
71	60.3	942.0	1.47E+06	663.6	3551.				0.10	0.433	60.00		THERMAL CALIBRATION	
72	60.3	1110.0	1.18E+06	659.6	3830.				0.10	0.443	60.00			
73	60.0	1107.0	1.16E+06	657.2	3820.				5.04	0.442	60.00			
74	60.3	1100.0	1.15E+06	659.0	3820.				-6.93	0.442	60.00			
75	60.5	1211.0	1.00E+06	657.0	3905.				0.07	0.451	60.00			
76	60.4	1981.0	8.49E+05	641.3	4263.				0.09	0.470	60.00			
77	36.1	1273.0	5.14E+05	377.0	3976.				0.10	0.519	60.00			
78	50.5	1310.0	6.64E+05	544.9	3972.				0.09	0.466	60.00			
79	70.6	1275.0	1.24E+06	760.4	3980.				0.10	0.438	60.00			
80	73.6	1224.0	1.14E+06	665.0	3977.				0.00	0.427	60.00			
81	100.3	1271.0	1.71E+06	1066.9	3976.				0.04	0.400	60.00			
82	73.9	1171.0	1.15E+06	644.3	3911.				0.06	0.433	60.00			
83	76.7	1150.0	1.06E+06	674.5	3866.				0.07	0.421	60.00			
84	60.1	1305.0	1.09E+06	655.0	3954.	10.0	10.00	7.50	0.11	0.450				
85	60.1	1441.0	8.44E+05	640.9	4251.	10.0	10.00	7.50	0.10	0.470				
86	70.3	1303.0	1.19E+06	762.7	3991.	10.0	10.00	7.50	0.10	0.439				
87	50.3	1220.0	8.56E+05	546.9	3961.	10.0	10.00	7.50	0.07	0.469				
88	10.2	1419.0	1.17E+05	127.6	4249.	30.0	21.00	7.50	0.10	0.341				1000-1100
89	21.9	1444.0	2.71E+05	170.1	4250.	30.0	21.00	7.50	0.07	0.340		1A	[illegible]	
90	60.1	300.0	4.27E+06	652.5	2661.	30.0	21.00	7.50	0.04	0.339		200A	14	225
91	41.2	301.0	4.15E+06	463.1	2631.	30.0	21.00	7.50	0.05	0.361		201B	60	225
92	36.1	301.0	1.77E+06	390.7	2630.	30.0	21.00	7.50	0.05	0.400		201C	720	
93	25.1	303.0	1.63E+06	292.0	2636.	30.0	21.00	7.50	0.06	0.423				
94	27.1	300.0	1.56E+06	307.7	2629.	30.0	21.00	7.50	0.04	0.416				
95	27.2	300.0	1.54E+06	306.5	2629.	30.0	21.00	7.50	0.06	0.416		9A	1012	
96	21.1	302.0	1.55E+06	305.6	2612.	30.0	21.00	7.50	0.05	0.416		9B	6070	
97	27.2	300.0	1.59E+06	300.1	2629.	30.0	21.00	7.50	0.02	0.416		9C	1330	
98	30.2	304.0	1.71E+06	340.0	2636.	30.0	21.00	7.50	0.04	0.400		1B	3120	
99	30.1	302.0	1.77E+06	340.7	2633.	30.0	21.00	7.50	0.04	0.407		1C	670	
100	73.4	304.0	4.49E+06	600.1	2636.				0.06	0.336	60.00	6A	3600	
101	61.0	309.0	4.50E+06	697.0	2640.				0.05	0.315	60.00	6B	3600	
102	41.0	302.0	4.33E+06	461.0	2613.	30.0	21.00	7.50	0.04	0.303		3A	92	
103	41.0	301.0	4.14E+06	469.7	2631.	30.0	21.00	7.50	0.05	0.303		3B	147	
104	49.0	1441.0	6.09E+05	576.6	4260.	30.0	21.00	7.50	0.05	0.409		2A	8	1120-1400
105	47.0	1416.0	6.04E+05	510.5	4269.	30.0	21.00	7.50	0.05	0.490		2B	7	
106	40.7	1417.0	6.04E+05	419.5	4260.	30.0	21.00	7.50	0.05	0.490		2C	3	
107	36.0	1414.0	7.16E+05	400.9	4261.	30.0	21.00	7.50	0.06	0.514		5A	5	

ORIGINAL PAGE IS
OF POOR QUALITY

ORIGINAL PAGE IS
OF POOR QUALITY

TABLE 2 (CONTINUED)

REF. 4 - TABLE VII RUN SCHEDULE (Continued)

	RUN	PT PSIA	TT DEG F	RE FT-1	Q PSF	V FT/SEC	SHOCK GENERATOR ANGLE DEG	SHOCK GENERATOR X,IN	SHOCK GENERATOR Y,IN	WEDGE DEG	B.L. THICK	FLAP	SAMPLE	TIME	TS_{MAX}, IR-TC °F
	108	26.8	[illegible]	[illegible]	288.6	4265.	30.0	31.00	7.50	0.08	0.553		5B	150	1000-1100
	109	27.0	[illegible]	[illegible]	288.0	4254.	30.0	31.00	7.50	0.04	0.551		5C	1967	
	110	27.0	[illegible]	[illegible]	288.7	4259.	30.0	31.00	7.50	0.07	0.552		6C	936	
	111	[illegible]	[illegible]	[illegible]	165.1	4250.	30.0	31.00	7.50	0.08	0.526		7A	51	
	112	[illegible]	[illegible]	[illegible]	164.4	4252.	30.0	31.00	7.50	0.06	0.526		7B	400	
	113	[illegible]	[illegible]	[illegible]	164.1	4250.	30.0	31.00	7.50	0.03	0.526		7C	850	
	114	[illegible]	[illegible]	[illegible]	407.0	4223.	30.0	31.00	7.50	0.04	0.513		3C	8	
	115	[illegible]	[illegible]	[illegible]	527.4	4248.	30.0	31.00	7.50	0.04	0.488		20	8615	
	116	[illegible]	[illegible]	[illegible]	741.5	4240.	30.0	31.00	7.50	0.08	0.466		20	915	
	117	[illegible]	[illegible]	[illegible]	528.1	4288.	30.0	31.00	7.50	0.04	0.489		30E	3614	
	118	33.0	[illegible]	[illegible]	381.6	4259.	30.0	16.00	7.50	0.08	0.527				
	119	16.0	1501.0	[illegible]	403.2	4254.	30.0	16.00	7.50	0.03	0.527		31B	91	1000-1100
	120	[illegible]	1441.0	[illegible]	360.8	4256.	30.0	16.00	7.50	0.04	0.530		311	110	
	121	[illegible]	[illegible]	[illegible]	300.8	4247.	30.0	16.00	7.50	0.04	0.527		31B	526	
	122	27.0	[illegible]	[illegible]	291.5	4257.	30.0	16.00	7.50	0.04	0.550		310	1736	
	123	27.0	[illegible]	[illegible]	289.5	4246.	30.0	16.00	7.50	0.06	0.551		31E	3035	
	124	32.7	[illegible]	[illegible]	350.7	4260.	30.0	16.00	7.50	0.04	0.520		10	451	
	125	[illegible]	[illegible]	[illegible]	360.7	4251.	30.0	16.00	7.50	0.03	0.527		11	21	
TC	126	[illegible]	[illegible]	[illegible]	360.5	4249.	30.0	16.00	7.50	0.06	0.521		13	1472	1000-1100
	127	[illegible]	[illegible]	[illegible]	362.4	4249.	30.0	16.00	7.50	0.05	0.527		14	18	
	128	[illegible]	[illegible]	[illegible]	350.5	4252.	30.0	16.00	7.50	0.05	0.520		15	110	
	129	34.1	[illegible]	[illegible]	364.8	4257.	30.0	16.00	7.50	0.06	0.526		31C	21	
	130	[illegible]	[illegible]	[illegible]	368.5	4260.	30.0	10.50	7.50	0.08	0.527		20	59	
	131	[illegible]	[illegible]	[illegible]	350.9	4240.	30.0	10.50	7.50	0.04	0.527		22	150	
	132	[illegible]	[illegible]	[illegible]	361.5	4250.	30.0	10.50	7.50	0.06	0.521		26	782	
	133	[illegible]	[illegible]	[illegible]	361.5	4250.	30.0	10.50	7.50	0.06	0.527		24	180	
TC	134	[illegible]	[illegible]	[illegible]	650.1	2636.	30.0	21.00	7.50	0.07	0.304		27	358	225
	135	41.4	[illegible]	[illegible]	661.7	2638.	30.0	21.00	7.50	0.06	0.304		30	176	
	136	[illegible]	[illegible]	[illegible]	650.8	2631.	30.0	21.00	7.50	0.06	0.304		30	60	
	137	78.7	1611.0	[illegible]	660.9	4244.	10.0	15.00	7.50	0.07	0.444		4A	27	1000-1100
	138	84.1	[illegible]	[illegible]	856.2	4251.	10.0	15.00	7.50	0.06	0.443		4B	874	
	139	[illegible]	[illegible]	[illegible]	319.2	4240.				0.06	0.540	60.00	4C	1450	
	140	27.2	1435.6	[illegible]	282.8	4244.	30.0	10.50	7.50	0.10	0.550		16	2650	
	141	[illegible]	1426.0	[illegible]	288.1	4236.	30.0	10.50	7.50	0.06	0.550		16	878	
	142	[illegible]	1461.0	[illegible]	363.8	4257.	30.0	10.50	7.50	0.11	0.526		16	24	
	143	[illegible]	[illegible]	[illegible]	640.8	4257.	0.0	0.00	0.00	0.11	0.444		4C	300	
	144	75.5	[illegible]	[illegible]	646.3	4251.				3.07	0.444	60.00	4C	900	
	145	[illegible]	[illegible]	[illegible]	851.3	4254.	10.0	13.60	7.50	3.07	0.444				
	146	[illegible]	[illegible]	[illegible]	840.7	4255.	10.0	13.60	7.50	3.07	0.444		4C	650	
	196	61.7	[illegible]	[illegible]	720.1	2631.	24.0	16.20	7.50	5.11	0.351		32B	60	
	197	61.1	[illegible]	[illegible]	719.4	2629.	24.0	16.20	7.50	5.12	0.350		21		
	198	[illegible]	[illegible]	[illegible]	717.7	2636.	24.0	16.20	7.50	5.12	0.350		34B		
	199	[illegible]	[illegible]	[illegible]	716.7	2635.	24.0	16.20	7.50	5.12	0.351		21		
	200	61.2	[illegible]	[illegible]	720.1	2633.	24.0	16.20	7.50	5.12	0.351		33A	15	
	201	[illegible]	[illegible]	[illegible]	718.1	2633.	24.0	16.20	7.50	5.12	0.351		33B		
	202	[illegible]	[illegible]	[illegible]	715.3	2631.	24.0	16.20	7.50	5.12	0.351		19		
	203	[illegible]	[illegible]	[illegible]	711.0	2631.	24.0	16.20	7.50	5.12	0.351		10	60	
	204	[illegible]	[illegible]	[illegible]	718.7	2635.	24.0	16.20	7.50	5.12	0.351		8A	3600	
	205	60.7	[illegible]	[illegible]	720.5	2629.	24.0	16.20	7.50	5.11	0.350		31F	60	225
	206	[illegible]	[illegible]	[illegible]	440.4	2620.	30.0	10.50	7.50	0.11	0.305		8B	1000	
	207	45.3	[illegible]	[illegible]	590.3	2627.	30.0	10.50	7.50	0.12	0.450		6B		
	208	44.7	1185.4	[illegible]	490.4	[illegible]	30.0	10.50	7.50	0.10	[illegible]		6B		
	209	27.0	[illegible]	[illegible]	394.4	2637.	21.0	10.50	7.50	0.07	0.417		THERM. CALIB.		
	210	[illegible]	[illegible]	[illegible]	381.2	3330.	21.0	16.50	7.50	0.07	0.480				
	211	[illegible]	902.0	[illegible]	380.1	3557.	21.0	16.50	7.50	0.06	0.497				
	212	[illegible]	1112.0	[illegible]	297.2	3831.	21.0	16.50	7.50	0.06	0.519				
	213	27.3	1215.0	[illegible]	290.1	3965.	21.0	16.50	7.50	0.06	0.520				
	214	27.0	1441.0	[illegible]	292.6	4251.	21.0	16.50	7.50	0.08	0.531				
	215	27.1	1157.0	[illegible]	293.7	3864.	21.0	16.50	7.50	5.07	0.521		31F	50	810-820
	216	27.2	1157.0	[illegible]	290.1	3864.	21.0	16.50	7.50	0.08	0.521		31F	1500	
	217	61.6	373.0	[illegible]	716.0	2795.	24.0	16.20	7.50	5.08	0.361		31G	60	225

ORIGINAL PAGE IS
OF POOR QUALITY

ORIGINAL PAGE IS
OF POOR QUALITY

TABLE VII RUN SCHEDULE

RUN	PT PSIA	TT DEG F	RE FT-1	Q PSF	V FT/SEC	SHOCK GENERATOR ANGLE DEG	SHOCK GENERATOR X,IN	SHOCK GENERATOR Y,IN	WEDGE DEG	B.L. THEOR	FLAP
1	37.5	296.0	1.58E+06	300.5	2623.				1.00	0.414	
2	37.5	296.0	1.58E+06	300.8	2622.				1.00	0.414	
3	37.4	298.0	1.57E+06	300.7	2625.				11.07	0.418	
4	37.4	298.0	1.58E+06	300.1	2625.				-8.96	0.418	
5	37.3	300.0	1.56E+06	300.1	2620.				1.08	0.415	
6	50.1	300.0	2.06E+06	562.0	2620.				1.07	0.360	
7	69.8	302.0	3.07E+06	782.6	2633.				1.07	0.348	
8	36.7	298.0	1.53E+06	301.0	2625.				-3.94	0.417	
9	38.0	948.0	6.30E+05	310.0	3613.				1.07	0.490	
10	51.1	336.0	1.18E+06	365.6	3591.				1.07	0.441	
11	30.3	299.0	1.74E+06	341.4	2627.				1.07	0.407	90.00
12	30.0	301.0	1.71E+06	330.0	2630.				-3.96	0.400	90.00
13	29.9	301.0	1.70E+06	336.3	2630.				6.04	0.400	90.00
14	29.8	300.0	1.71E+06	335.0	2629.				11.03	0.400	90.00
15	30.0	301.0	1.71E+06	337.9	2630.				0.02	0.400	80.00
16	29.9	299.0	1.72E+06	337.3	2627.				0.01	0.408	60.00
17	30.0	298.0	1.72E+06	337.9	2625.				0.01	0.407	70.00
18	26.1	300.0	1.13E+06	276.6	2642.				0.02	0.443	60.00
19	39.3	300.0	2.29E+06	442.4	2620.				0.01	0.386	60.00
20	59.9	298.0	3.48E+06	672.8	2626.				0.01	0.365	60.00
21	69.7	300.0	3.90E+06	781.8	2620.				0.01	0.365	60.00
22	79.5	296.0	4.57E+06	890.8	2622.				0.00	0.335	60.00
23	59.9	900.0	1.42E+06	663.3	3549.				-0.00	0.424	60.00
24	59.7	899.0	1.41E+06	661.6	3547.				-3.93	0.424	60.00
25	30.0	302.0	1.71E+06	337.9	2632.	40.0	6.00	8.00	3.00	0.400	60.00
26	30.1	303.0	1.71E+06	330.6	2634.	30.0	6.00	8.00	3.00	0.400	60.00
27	29.8	303.0	1.69E+06	335.5	2634.	30.0	13.00	7.50	3.00	0.409	60.00
28	29.9	304.0	1.70E+06	336.5	2636.	30.0	13.00	7.50	7.05	0.409	
29	29.9	304.0	1.69E+06	336.2	2636.	30.0	13.00	7.50	-2.92	0.409	
30	30.2	302.0	1.72E+06	340.3	2632.	12.0	15.10	7.50	0.09	0.400	
31	29.9	300.0	1.71E+06	336.2	2629.	18.0	18.60	7.50	0.08	0.408	
32	22.1	301.0	1.26E+06	249.2	2630.	18.0	18.60	7.50	0.07	0.434	
33	40.0	300.0	2.29E+06	450.0	2629.	18.0	18.60	7.50	0.07	0.385	
34	46.3	302.0	2.64E+06	520.5	2633.	18.0	18.60	7.50	0.08	0.374	
35	49.8	300.0	2.84E+06	550.9	2629.	18.0	18.60	7.50	0.08	0.369	
36	59.7	300.0	3.41E+06	649.5	2629.	18.0	18.60	7.50	0.08	0.356	
37	80.0	300.0	4.56E+06	896.5	2629.	18.0	18.60	7.50	0.07	0.335	
38	79.8	301.0	4.55E+06	895.1	2631.	18.0	18.60	7.50	0.03	0.336	
39	80.0	298.0	4.58E+06	896.8	2626.	30.0	21.60	7.50	0.04	0.335	
40	70.0	282.0	4.19E+06	785.2	2598.	30.0	21.00	7.50	0.07	0.342	
41	58.2	276.0	3.49E+06	653.2	2587.	30.0	21.00	7.50	0.06	0.354	
42	51.2	302.0	2.91E+06	575.1	2633.	30.0	21.00	7.50	0.06	0.367	
43	40.6	314.0	2.26E+06	456.6	2653.	30.0	21.00	7.50	0.05	0.386	
44	29.8	307.0	1.68E+06	335.9	2641.	30.0	21.00	7.50	0.05	0.400	
45	20.2	301.0	1.15E+06	227.8	2630.	30.0	21.00	7.50	0.06	0.442	
46	50.3	916.0	1.17E+06	956.6	3570.	30.0	21.00	7.50	0.06	0.440	
47	100.3	907.0	2.35E+06	1107.6	3559.				0.06	0.303	60.00
48	30.0	1211.0	5.19E+05	327.8	3960.				0.06	0.510	60.00
49	60.0	1195.0	1.09E+06	652.4	3941.				0.06	0.450	60.00
50	59.8	1446.0	8.36E+05	636.9	4259.				-0.94	0.471	60.00

B.L. SURVEY

PRESSURE CALIBRATION

ORIGINAL PAGE IS
OF POOR QUALITY

TABLE 2 (CONCLUDED)

REF. 4 - TABLE VII RUN SCHEDULE (Continued)

RUN	PT PSIA	TT DEG F	RE FT-1	Q PSF	V FT/SEC	SHOCK GENERATOR ANGLE DEG	SHOCK GENERATOR X,IN	SHOCK GENERATOR Y,IN	WEDGE DEG	B.L. THICK	FLAP	SAMPLE	TIME	TS_{MAX}, °F IR
318	61.7	270.4	1.19E+06	715.6	2701.	34.0	16.20	7.90	5.00	0.362		313	60	225
319	62.6	301.5	[illegible]	713.9	2631.	30.4	16.20	7.90	5.05	0.351		64		"
320	61.7	301.4	[illegible]	715.2	2631.	30.0	16.20	7.90	5.05	0.351		169		
322	76.9	1107.4	4.970E+05	295.4	3071.	31.0	16.50	7.90	0.05	0.522		313	1200	
323	76.9	1195.4	[illegible]	295.7	[illegible]	31.0	16.50	7.90	0.06	0.522		10		
324	76.8	1255.4	4.130E+05	291.5	4022.	41.0	16.50	7.90	0.05	0.535		10		
325	76.9	1301.4	4.440E+05	292.1	4026.	31.0	16.50	7.90	0.06	0.534		317		
326	71.0	1250.6	4.470E+05	293.7	4047.	31.0	16.50	7.90	0.06	0.534		318		
327	76.9	1237.4	4.440E+05	291.4	4025.	31.0	16.50	7.90	0.05	0.534		313		
328	70.1	1043.0	5.720E+05	287.0	4277.	41.0	16.50	7.90	0.06	0.350		313		
329	76.9	1059.0	[illegible]	294.2	4200.	31.0	16.50	7.90	0.00	0.351		317		
330	71.4	1004.4	[illegible]	409.5	4230.	31.0	16.50	7.90	0.00	0.351		316		
331	74.9	1004.4	[illegible]	400.5	4250.	31.0	16.50	7.90	0.05	0.351		10		
332	77.3	[illegible]	[illegible]	784.4	3040.	34.0	16.20	7.90	5.06	0.353		12	60	
333	76.9	1141.6	[illegible]	290.3	3877.	31.0	16.50	7.90	5.00	0.521		12	208	
334	76.9	1162.4	4.970E+05	295.4	3871.	31.0	16.50	7.90	0.07	0.522		12	994	
335	77.2	1210.0	4.401E+05	295.1	4034.	41.0	16.50	7.90	0.04	0.536		12	1200	
336	76.9	1567.0	4.710E+05	291.0	4703.	31.0	16.50	7.90	0.05	0.356		12	1200	
331	37.	1133.				31.	16.5	7.5	0.			310		

TABLE 2 (CONCLUDED)

REP. 4 - TABLE VII RUN SCHEDULE (Continued)

RUN	PT PSIA	TT DEG F	RE FT-1	Q PSF	V FT/SEC	SHOCK GENERATOR ANGLE DEG	SHOCK GENERATOR X,IN	SHOCK GENERATOR Y,IN	WEDGE DEG	B.L. THROAT	FLAP	SAMPLE	TIME	TS_{MAX}, °F IR
218	61.7	374.0	[illegible]	315.6	2765.	24.0	16.20	7.50	5.05	0.362		31J	60	225
219	63.6	381.6	[illegible]	313.0	2631.	24.0	16.20	7.50	5.05	0.351		6A		
220	63.7	381.0	[illegible]	315.2	2631.	24.0	16.20	7.50	5.05	0.351		16A		
222	26.4	1142.0	[illegible]	295.4	3871.	31.0	16.50	7.50	0.05	0.522		31J	1200	
223	26.5	1155.0	[illegible]	295.7	3862.	21.0	16.50	7.50	0.06	0.522		10		
224	26.8	1254.0	[illegible]	291.5	4022.	21.0	16.50	7.50	0.08	0.536		10		
225	26.4	1301.0	[illegible]	292.3	4024.	21.0	16.50	7.50	0.06	0.534		31F		
226	21.0	1259.6	[illegible]	293.7	4023.	21.0	16.50	7.50	0.06	0.534		31G		
227	26.9	1272.6	[illegible]	293.6	4025.	21.0	16.50	7.50	0.05	0.536		31J		
228	20.7	1402.0	[illegible]	287.6	4277.	21.0	16.50	7.50	0.06	0.550		31J		
229	28.9	1436.0	[illegible]	286.2	4269.	21.0	16.50	7.50	0.05	0.551		31F		
230	21.6	1440.0	[illegible]	289.5	4250.	21.0	16.50	7.50	0.06	0.551		31G		
231	26.9	1444.0	[illegible]	288.5	4250.	21.4	16.50	7.50	0.05	0.551		10		
232	67.3	815.0	[illegible]	303.6	3638.	24.0	16.20	7.50	5.06	0.353		13	60	
233	26.4	1163.0	[illegible]	296.7	3877.	21.0	16.50	7.50	5.06	0.521		13	308	
234	26.5	1162.0	[illegible]	295.4	3871.	21.0	16.50	7.50	0.07	0.522		13	992	
235	27.2	1261.0	[illegible]	295.7	4034.	21.0	16.50	7.50	0.06	0.536		13	1200	
236	26.9	1312.0	[illegible]	287.6	4703.	21.0	16.50	7.50	0.05	0.556		13	1200	
221	37.	1135.				31.	16.3	7.3	0.			31G		

ORIGINAL PAGE IS
OF POOR QUALITY

ORIGINAL PAGE IS
OF POOR QUALITY

TABLE 3

PRESSURE FLUCTUATIONS (PSI) DOWNSTREAM OF SHAFT

TRANSDUCER #1 (1-inch downstream of shaft centerline)

Ps (psi) \ RPS	0	100	200	300
.02	.034	.036	.040	.043
.05	.060	.061	.065	.072
.1	.097	.095	.099	.105
.2	.164	.139	.155	.180
.3	.201	.188	.202	.228
.4	.225	.225	.234	.240
.5	.304	.335	.316	.316
.6	.348	.417	.398	.386
.7	.386	.433	.408	.398
.8	.664	.711	.686	.658

TRANSDUCER #2 (1 1/2-inches downstream of shaft centerline)

.02	.027	.030	.033	.036
.05	.050	.053	.056	.060
.1	.081	.082	.085	.092
.2	.149	.117	.130	.145
.3	.183	.158	.177	.196
.4	.202	.183	.198	.209
.5	.225	.243	.237	.240
.6	.243	.272	.269	.275
.7	.269	.285	.281	.285
.8	.364	.493	.471	.477

TRANSDUCER #3 (1-inch downstream and 1/4-inch above shaft centerline)

.02	.024	.029	.034	.035
.05	.041	.046	.050	.055
.1	.070	.073	.075	.082
.2	.126	.114	.133	.164
.3	.171	.168	.187	.212
.4	.218	.206	.218	.231
.5	.285	.316	.313	.307
.6	.316	.386	.370	.329
.7	.354	.402	.383	.373
.8	.582	.617	.604	.594

[redacted]

TABLE 3 (CONCLUDED)

OVERALL SOUND PRESSURE LEVELS (DB) DOWNSTREAM OF SHAFT

TRANSDUCER #1 (1-inch downstream of shaft centerline)

RPS / Ps(psi)	0	100	200	300
.02	142	142	143	144
.05	147	147	147	148
.1	151	151	151	151
.2	155	154	155	156
.3	157	156	157	158
.4	158	158	158	159
.5	161	162	161	161
.6	162	163	163	163
.7	163	164	163	163
.8	167	168	168	167

TRANSDUCER #2 (1 1/2-inches downstream of shaft centerline)

.02	140	141	141	142
.05	145	146	146	147
.1	149	149	150	150
.2	154	152	153	154
.3	156	155	156	157
.4	157	156	157	157
.5	158	159	159	159
.6	159	160	160	160
.7	160	160	160	160
.8	162	165	164	165

TRANSDUCER #3 (1-downstream and 1/4-inch above shaft centerline)

.02	139	140	142	142
.05	143	144	145	146
.1	148	148	149	149
.2	153	152	153	155
.3	156	155	156	158
.4	158	157	158	158
.5	160	161	161	161
.6	161	163	162	161
.7	162	163	163	162
.8	166	167	167	166

TABLE 4

AFRSI THREAD TIMES TO FAILURE

AFRSI THREAD ANALYSIS: .031" LOOP
THREAD CONDITION: HEAT CLEANED (650F/4HRS, 850F/2HRS)

TEST	.4,200	.4,300	.5,100	.5,200	.5,300	.6,100	.6,200	.6,300
DATA	282	1154	1800	355	130	1800	476	130
	1800	1615	1800	750	464	1800	216	86
	1370	1532	1800	342	259	708	58	13
	1800	1800	310	182	95	180	147	15
	256	1800	1635	366	145	545	47	19
	1800	1800	1800	461	280	1021	498	178
	1800	1800	1800	400	161	1609	94	152
	1800	1800		1198	392	1800	40	52
	1400	1050		1800	175	1800	89	
	1800	1800		276	90	1800	238	
	1800	1800		554	21	1800	427	
		440		1478	760		85	
		290		247	900			
				199	90			
				1743	47			
				1174				
				1800				
				805				
				1800				
				1349				
COUNT	11	13	7	20	15	11	12	8
MAX	1800	1800	1800	1800	900	1800	498	178
MIN	256	290	310	182	21	180	40	13
MEAN	1446	1437	1564	864	267	1351	201	81
ST DEV	605	540	556	612	261	618	172	66
MEAN N	289236	431100	156357	172790	80180	135118	40250	24188
STDEV N	120931	162078	55618	122470	78268	61801	34481	19816

TABLE 4 (CONTINUED)

AFRSI THREAD TIMES TO FAILURE

AFRSI THEAD ANALYSIS: .031" LOOP
THREAD CONDITION: HEAT CLEANED + ENTRY
(650F/4HRS,850F/2HRS,1200F/10MIN)

TEST	.02,50	.02,100	.02,200	.05,50	.05,100	.1,50	.1,100
DATA	525	145	8	170	3	2	0
	400	355	105	11	8	3	0
	475	169	41	78	5	2	0
	286	48	65	65	9	1	
	119	97	4	18	5		
	274			52	2		
	130			11			
	640			1			
	802			44			
	1559			129			
	162			24			
	568			33			
	89			2			
				4			
				1			
				2			
				3			
				3			
				2			
				18			
				3			
COUNT	13	5	5	21	6	4	3
MAX	1559	355	105	170	9	3	0
MIN	89	48	4	1	2	1	0
MEAN	464	163	45	32	5	2	0
ST DEV	397	117	42	46	3	1	0
MEAN N	23188	16280	8920	1605	533	100	0
ST DEV N	19860	11705	8405	2277	273	41	0

ORIGINAL PAGE IS
OF POOR QUALITY

TABLE 4 (CONCLUDED)

AFRSI THREAD TIMES TO FAILURE

AFRSI THREAD ANALYSIS: .031" LOOP
THREAD CONDITION: OFF SPOOL

TEST	.5,300	.6,300	.7,300	.8,200	.8,300
DATA	1800	340	996	1800	686
	1800	485	870	1800	456
	1800	1050	650	1800	500
		1800	1630		420
		1800			1000
					572
COUNT	3	5	4	3	6
MAX	1800	1800	1630	1800	1000
MIN	1800	340	650	1800	420
MEAN	1800	1095	1037	1800	606
ST DEV	0	696	421	0	215
MEAN N	540000	328500	310950	360000	181700
ST DEV N	0	208829	126213	0	64500

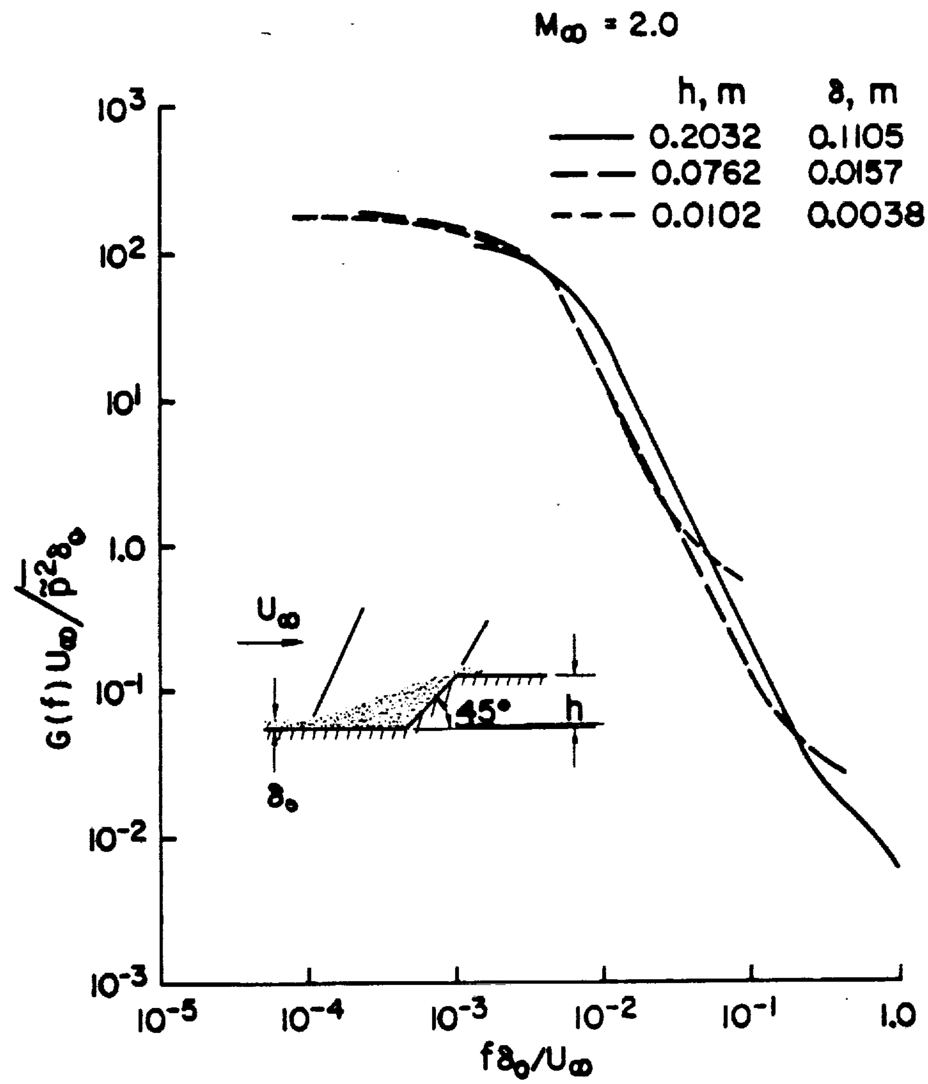

Figure 1.- Scaling of power spectral densities of pressure fluctuations due to shock waves.

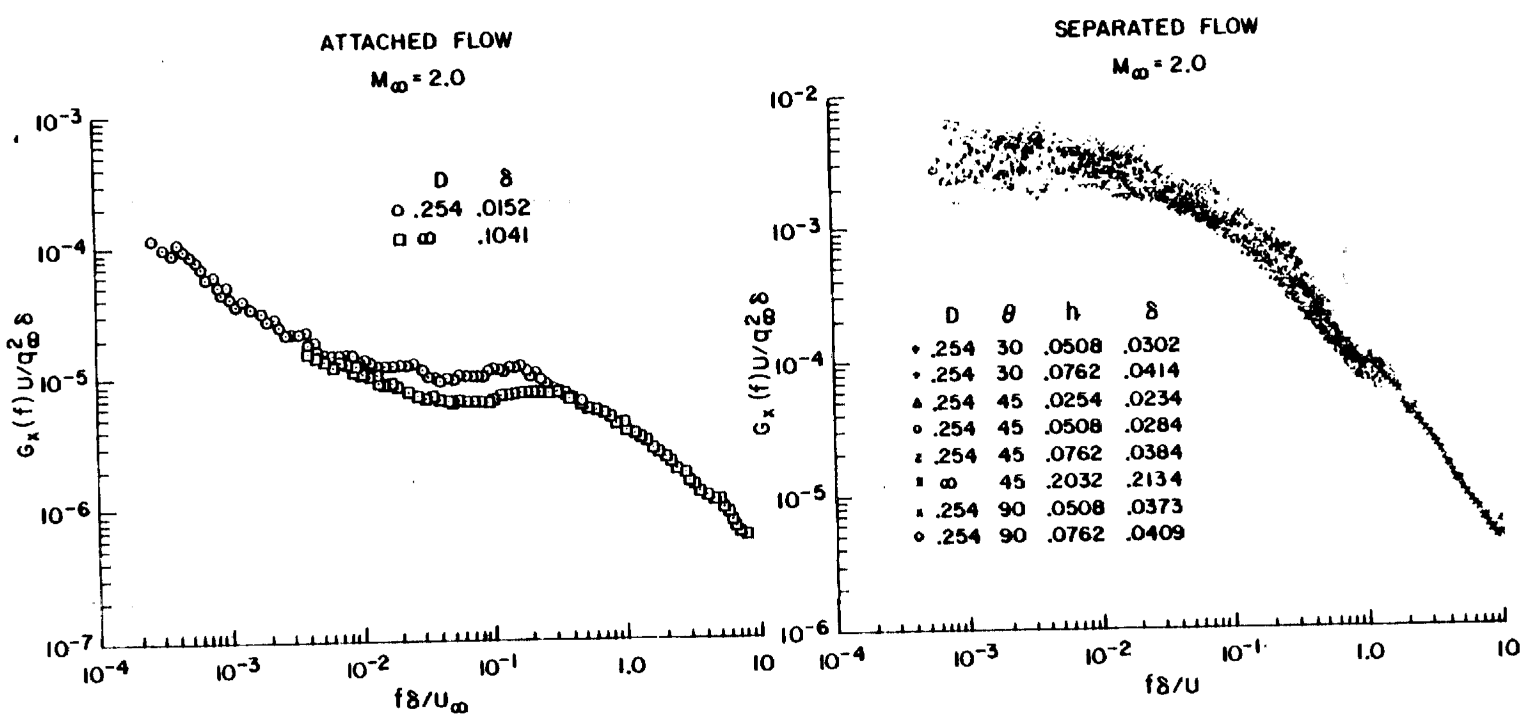

Figure 2.- Scaling of power spectral densities of pressure fluctuations due to attached and separated turbulent boundary layers.

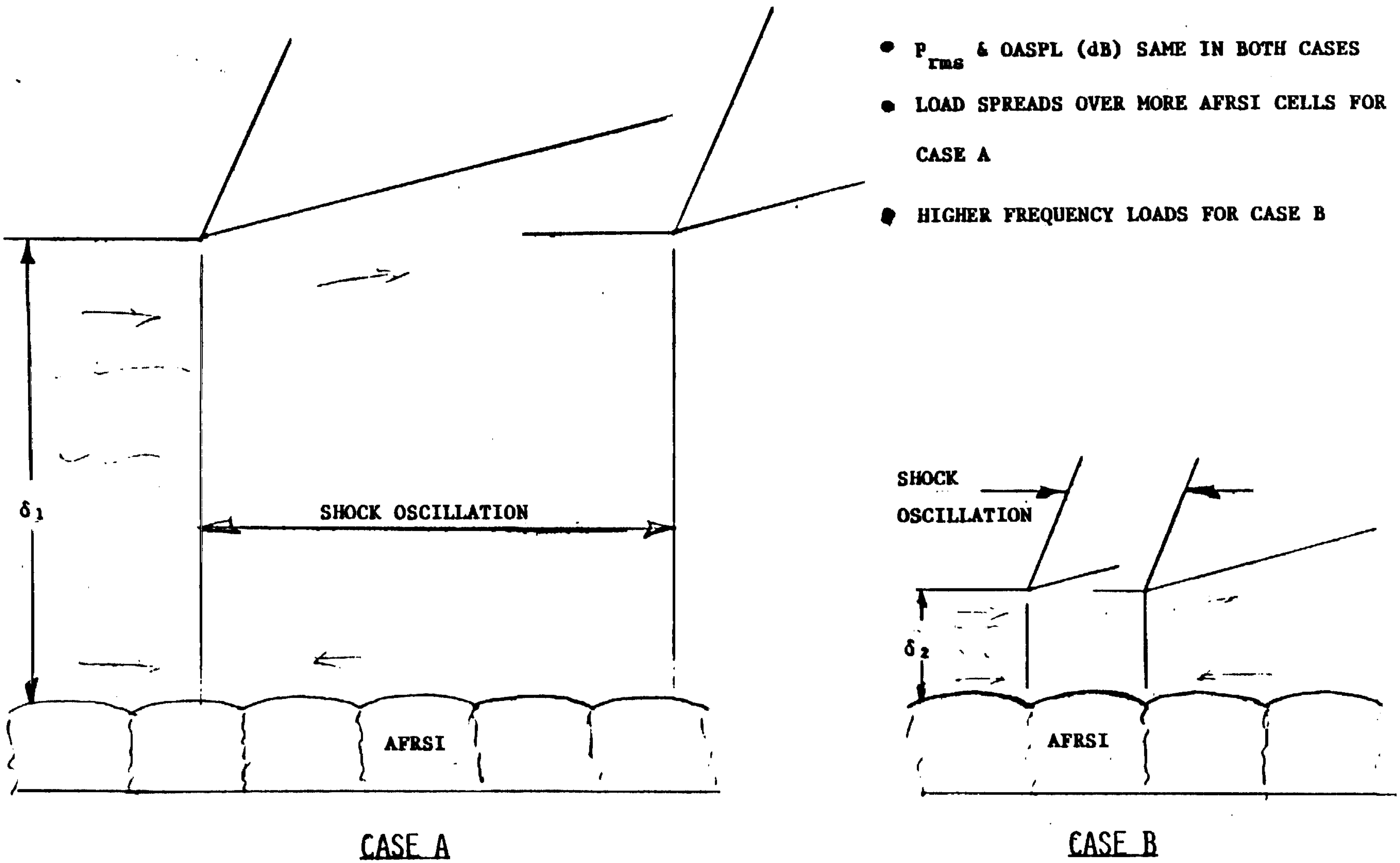

Figure 3.- Effects of boundary-layer thickness on the scaling of pressure fluctuations due to shock waves on AFRSI.

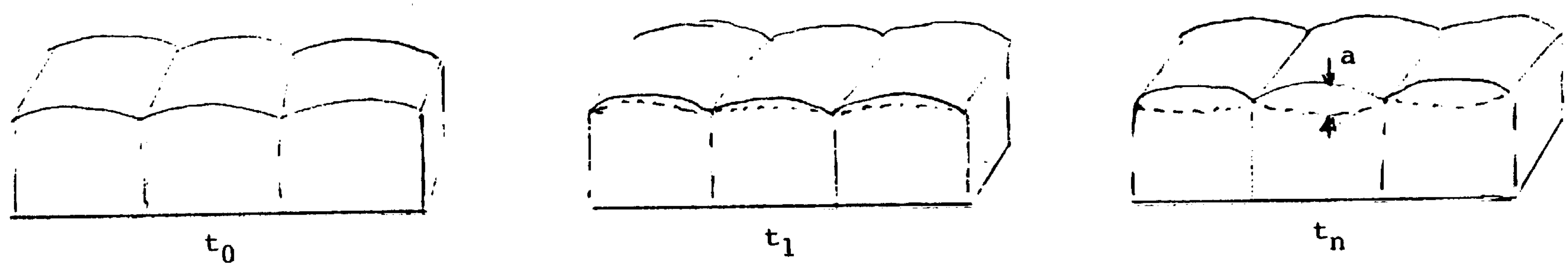

- FILLER MATERIAL HAS LOW RESILIENCY.
- FILLER MATERIAL COMPRESSES WITH EACH CYCLE OF OSCILLATION.
- AMPLITUDES, THUS CURVATURE OF CLOTH, SELF ABRASION AND FILAMENT FRACTURE, INCREASE WITH EACH CYCLE OF OSCILLATION.
- FOR SAME ΔP AND dB LEVEL, THIN BOUNDARY LAYERS COMPRESS FILLER MATERIAL MORE RAPIDLY THAN THICK BOUNDARY LAYERS.

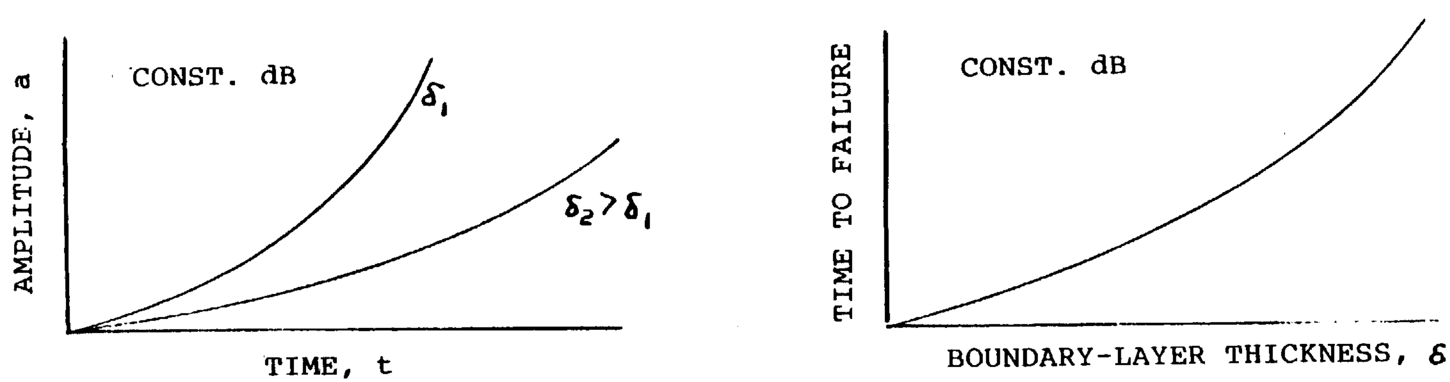

ORIGINAL PAGE IS OF POOR QUALITY

Figure 4.- A hypothesis of AFRSI failures and the effects of boundary-layer thickness.

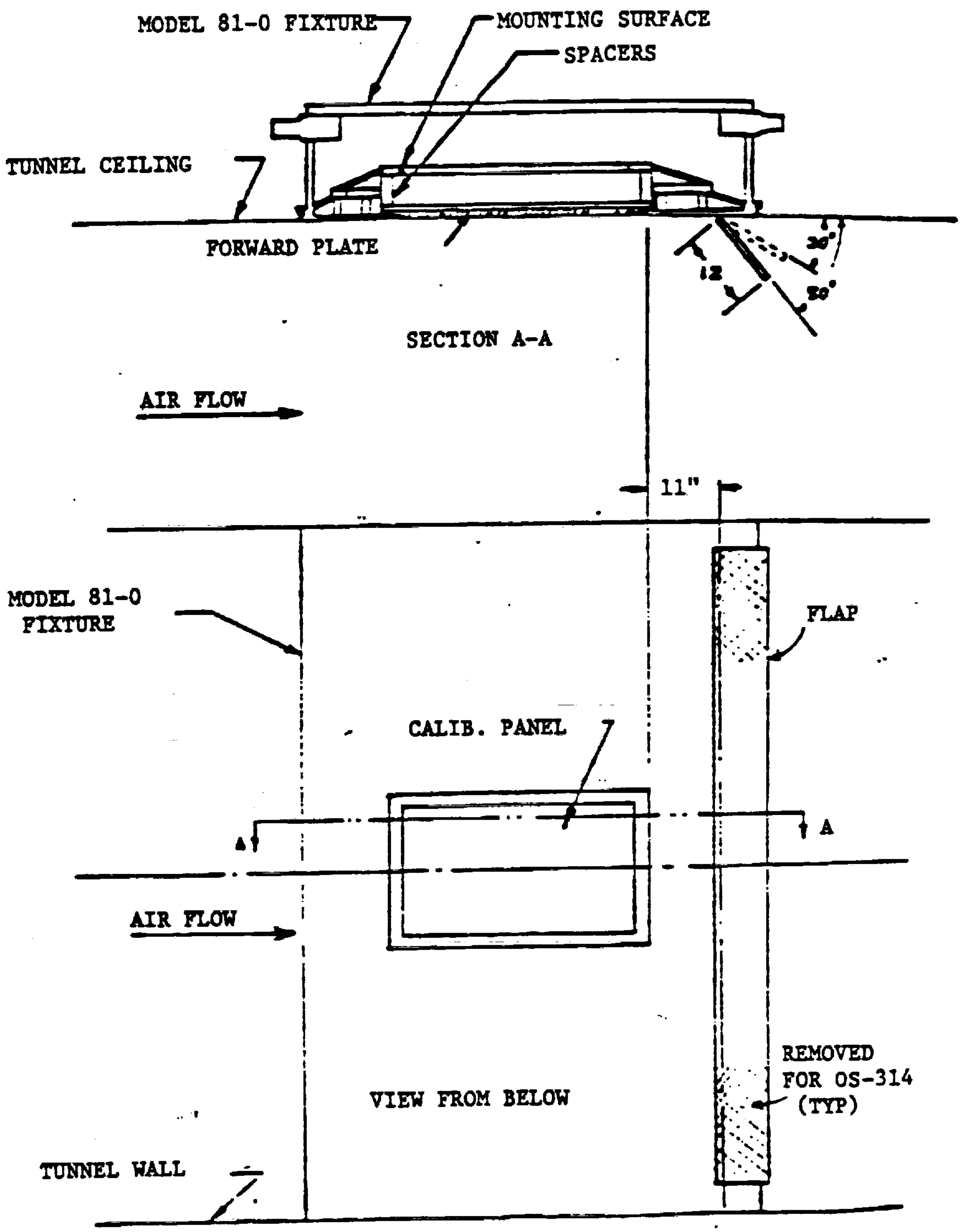

Figure 5.- OS-314 test fixture installation in Ames 9-x 7-Foot Supersonic Wind Tunnel.

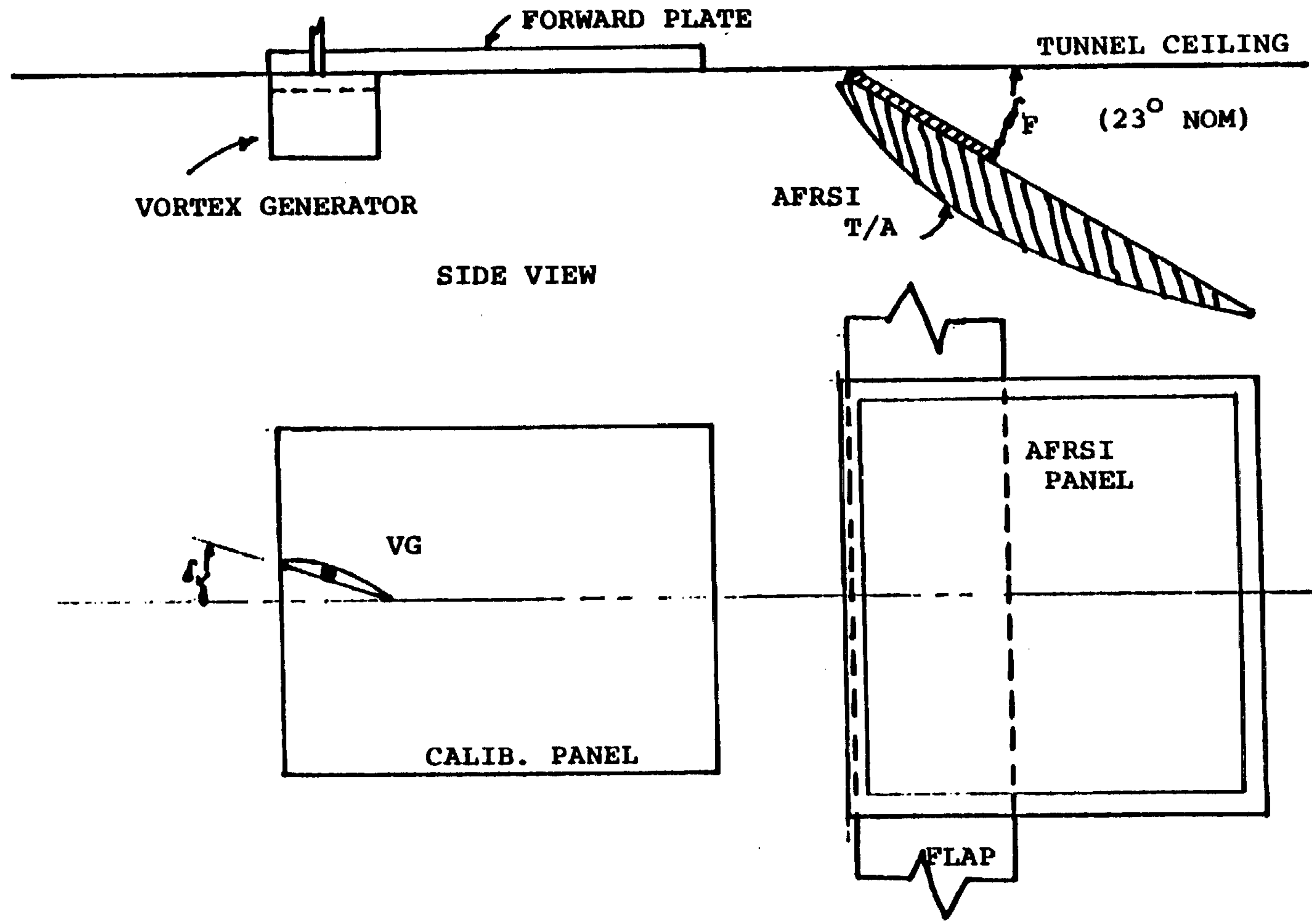

VIEW LOOKING AT CEILING

FIGURE 6.- TEST INSTALLATION SCHEMATIC (OS-314)

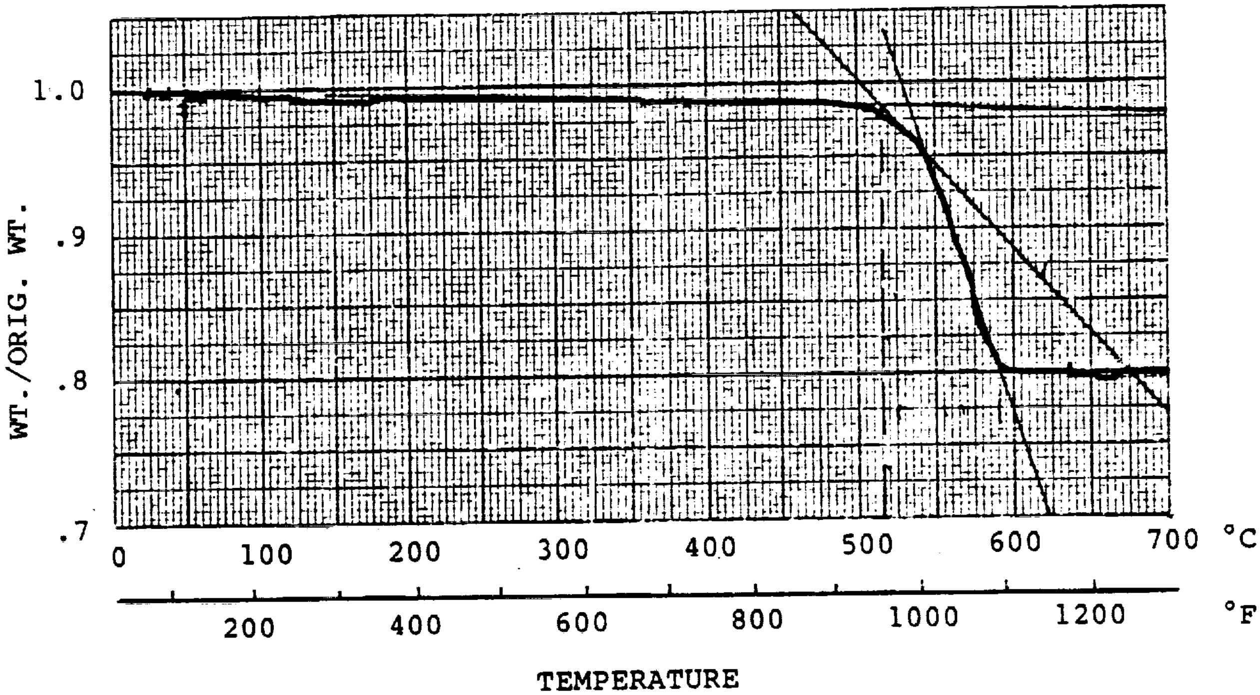

(a) Thread off spool

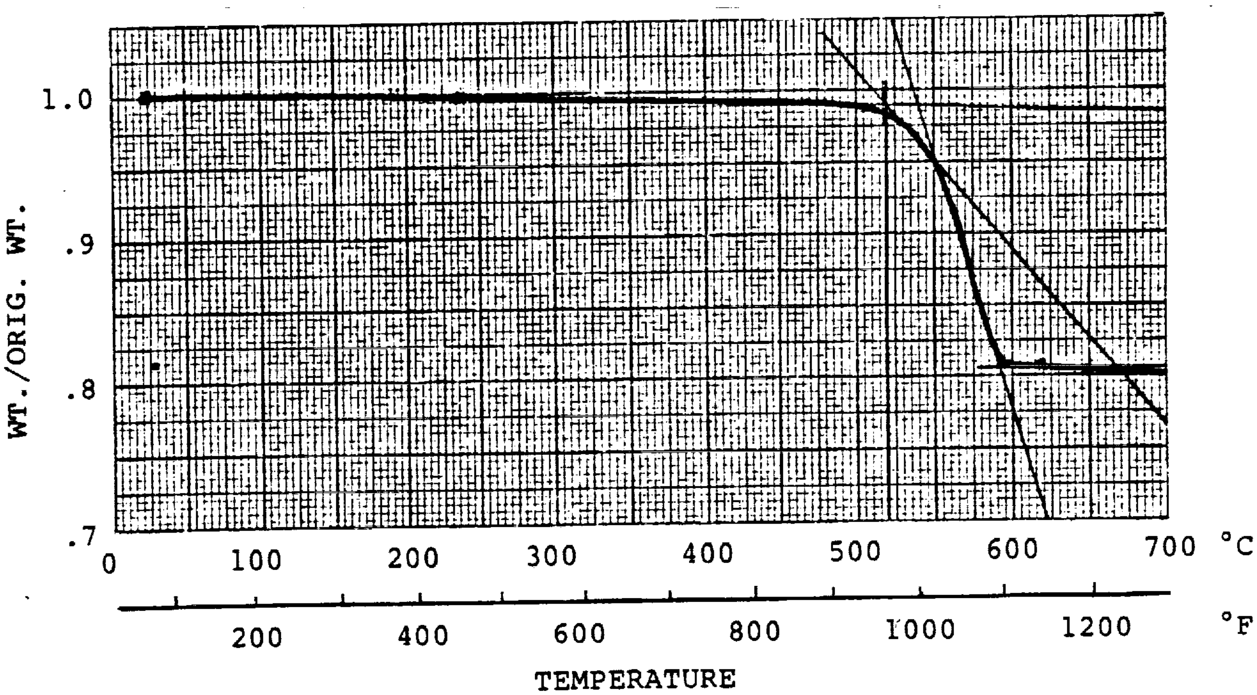

(b) Thread heat cleaned (4hrs @ 650°F, 2hrs @ 850°F)

Figure 7.- Thermo gravimetric analysis if AFRSI threads.

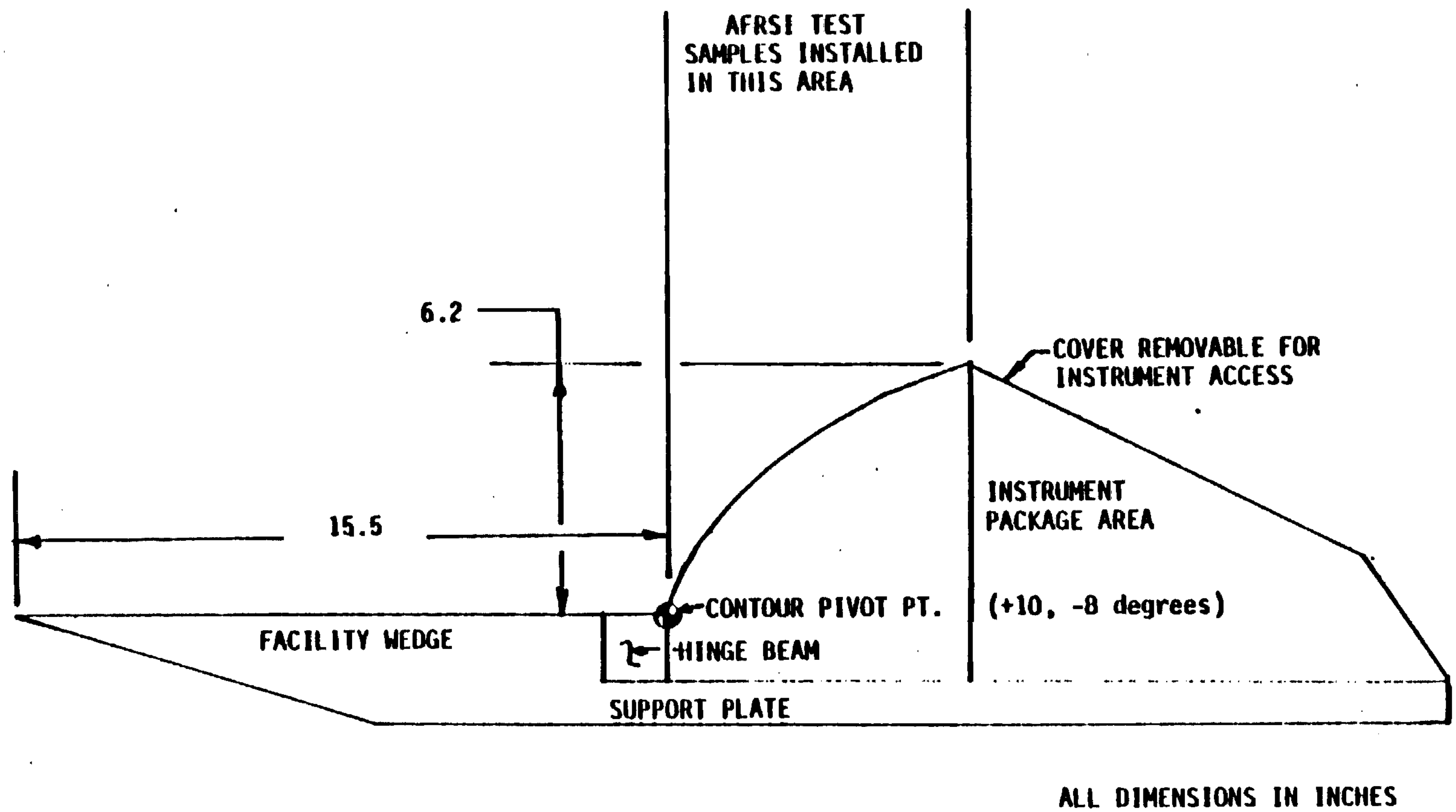

Figure 8.- OS-315 test fixture.

COMPARISON OF 1/3 OCTAVE SPECTRA FROM ARC AND AEDC

OASPL = 158 dB

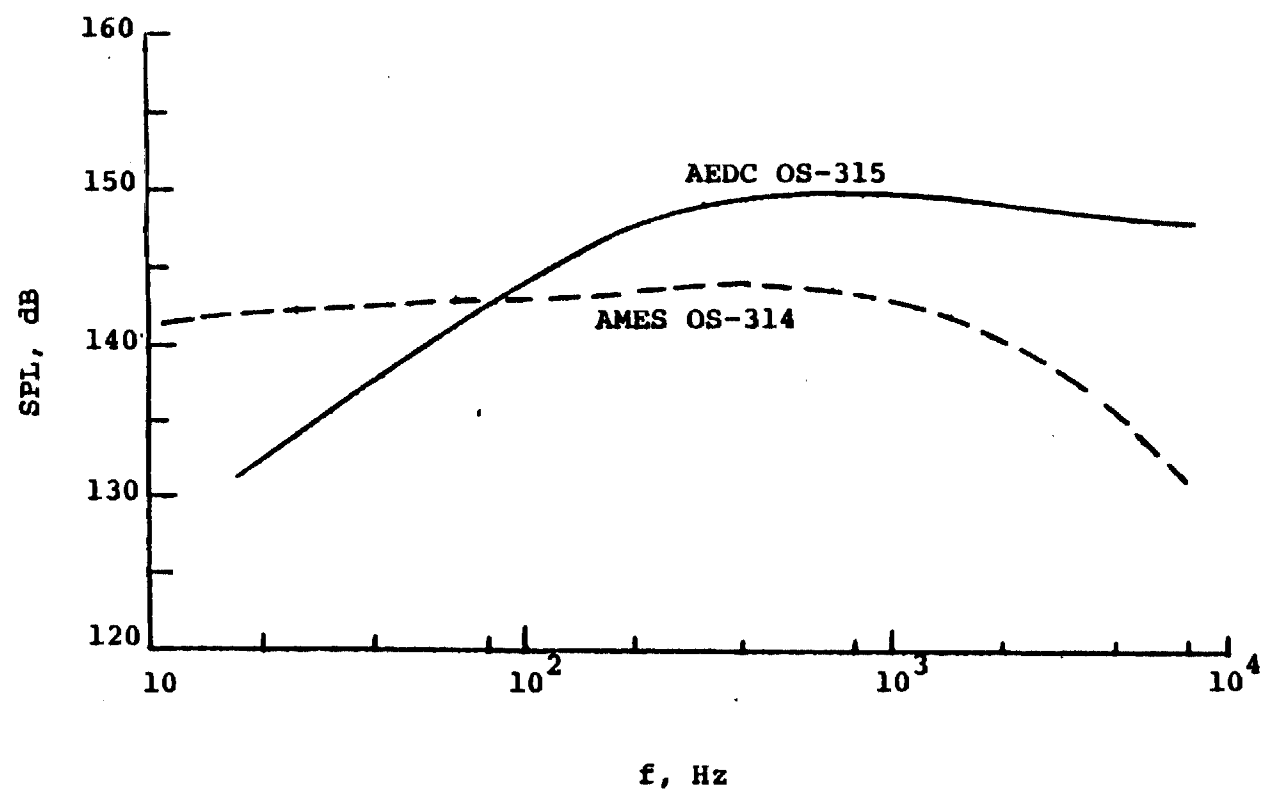

Figure 9.- Comparisons of one-third octave spectra of pressure fluctuations from OS-314 and OS-315 with OASPLs=160.4.

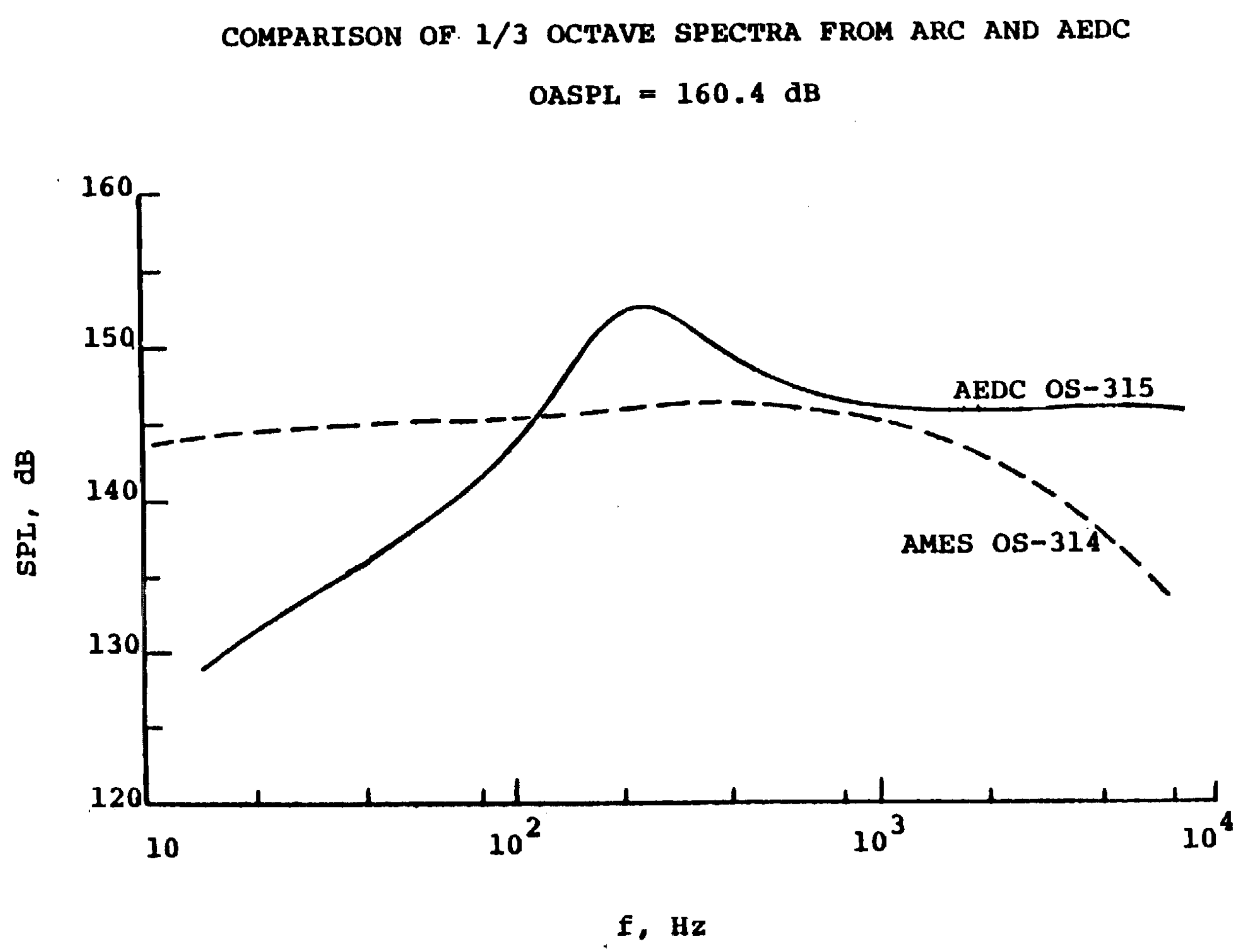

Figure 10.- Comparisons of one-third octave spectra of pressure fluctuations from OS-314 and OS-315 with OASPLs= 158 dB.

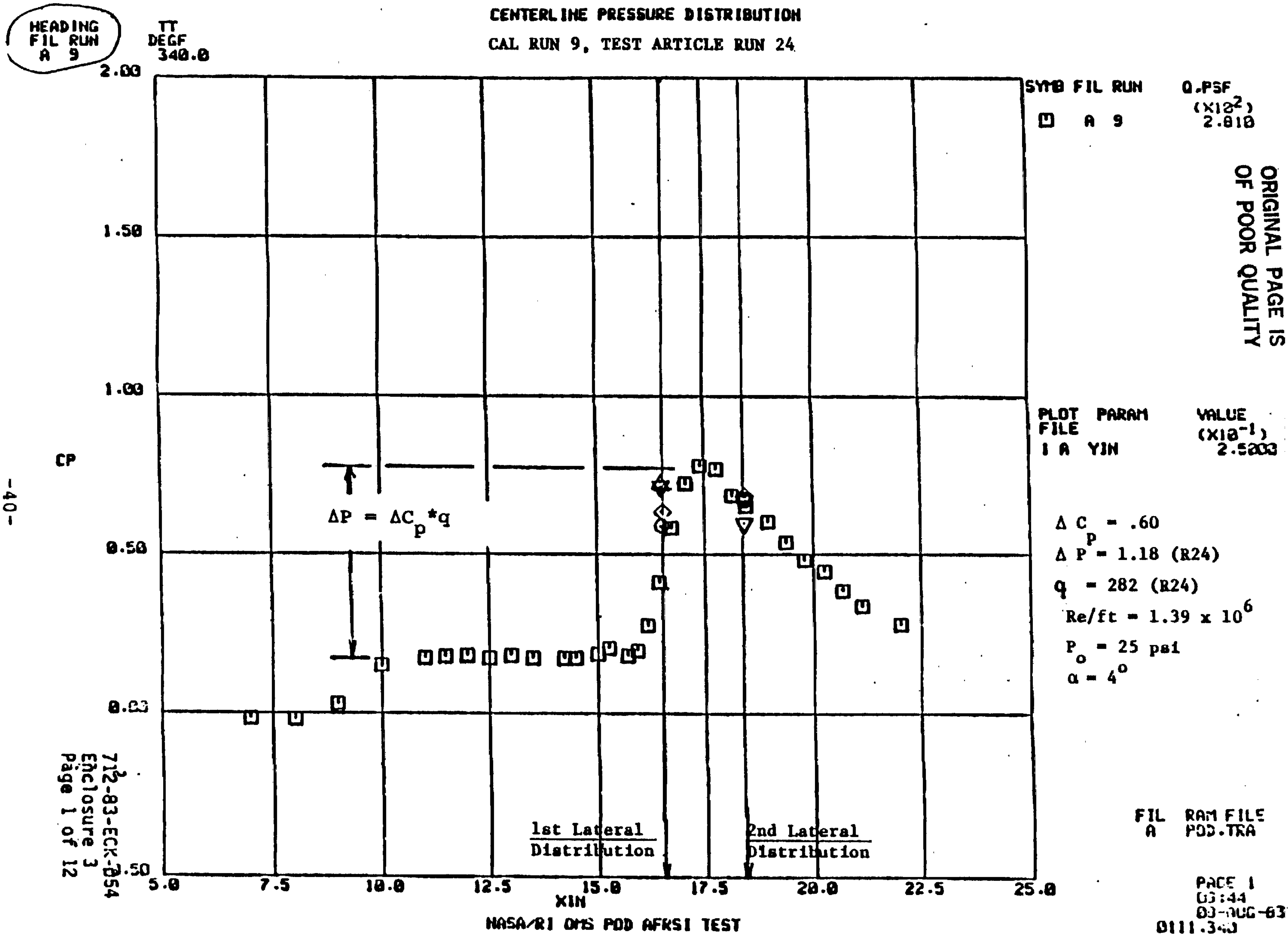

Figure 11. Static pressure distribution on OS-315 fixture for ascent simulation, TT=340°F.

712-83-ECK-054
Enclosure 3
Page 1 of 12

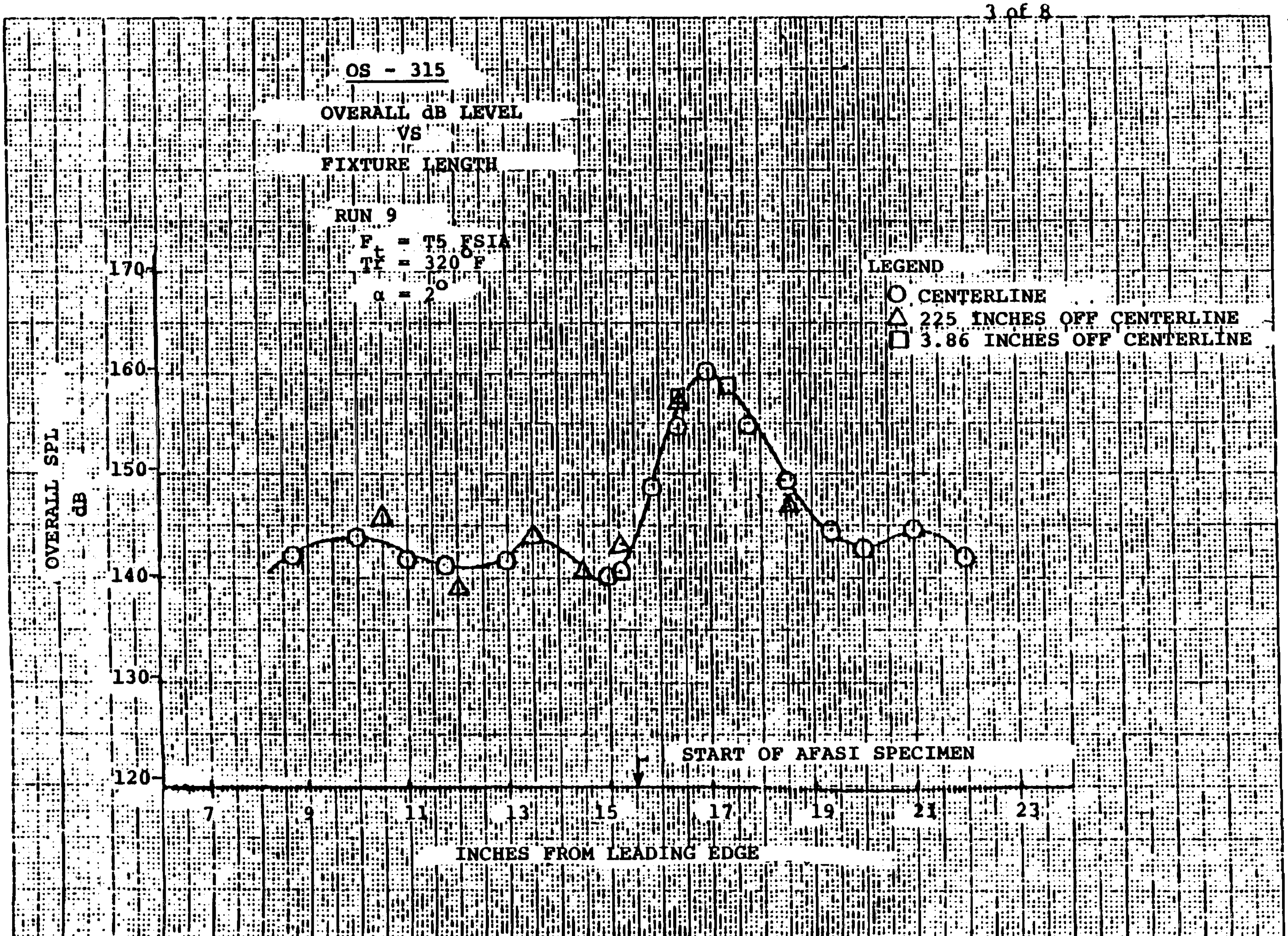

Figure 12. OASPLs on OS-315 fixture for ascent simulation, TT=340°F.

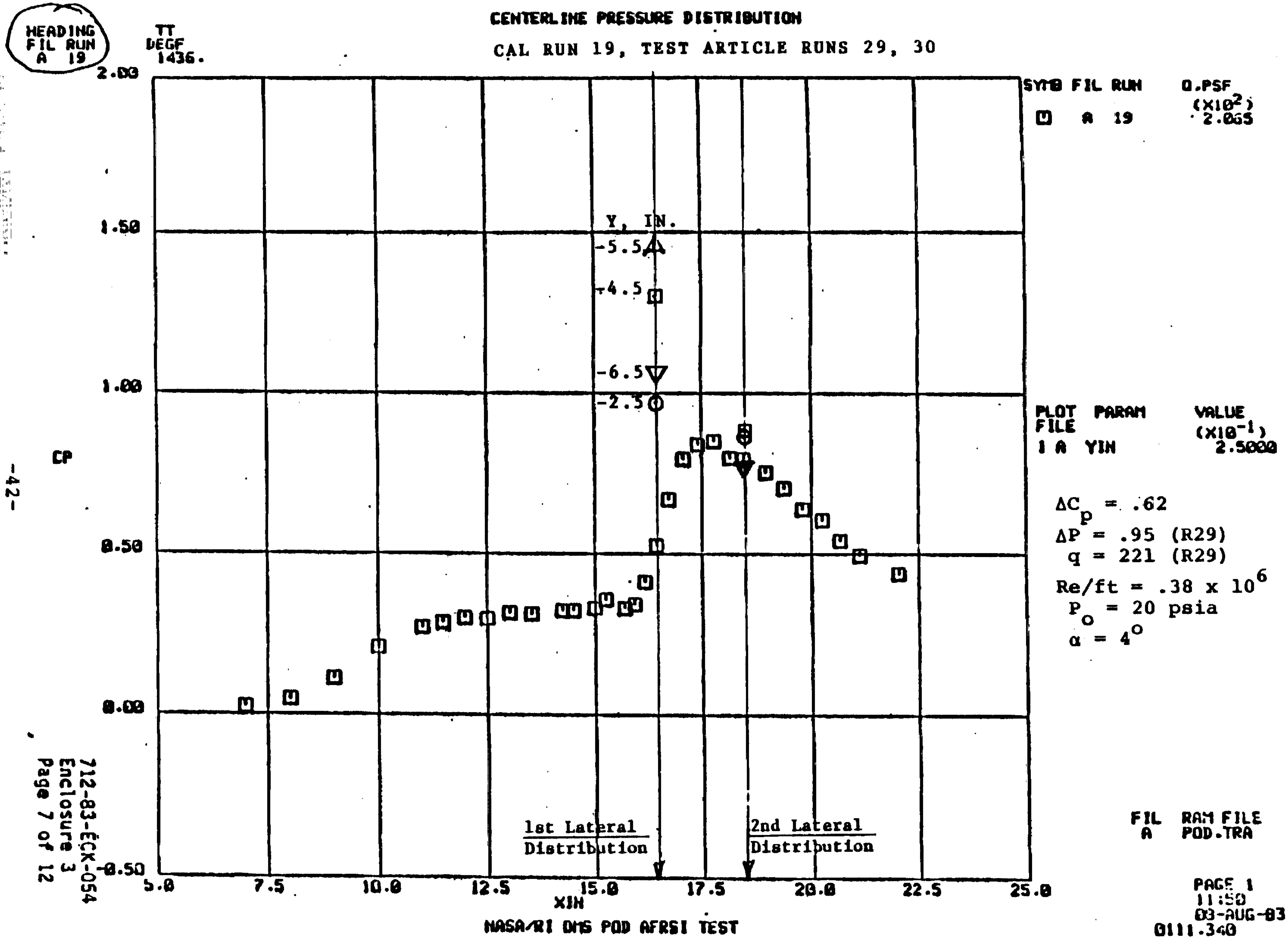

Figure 13.- Static pressure distribution on OS-315 fixture for entry simulation, TT=1,436°F.

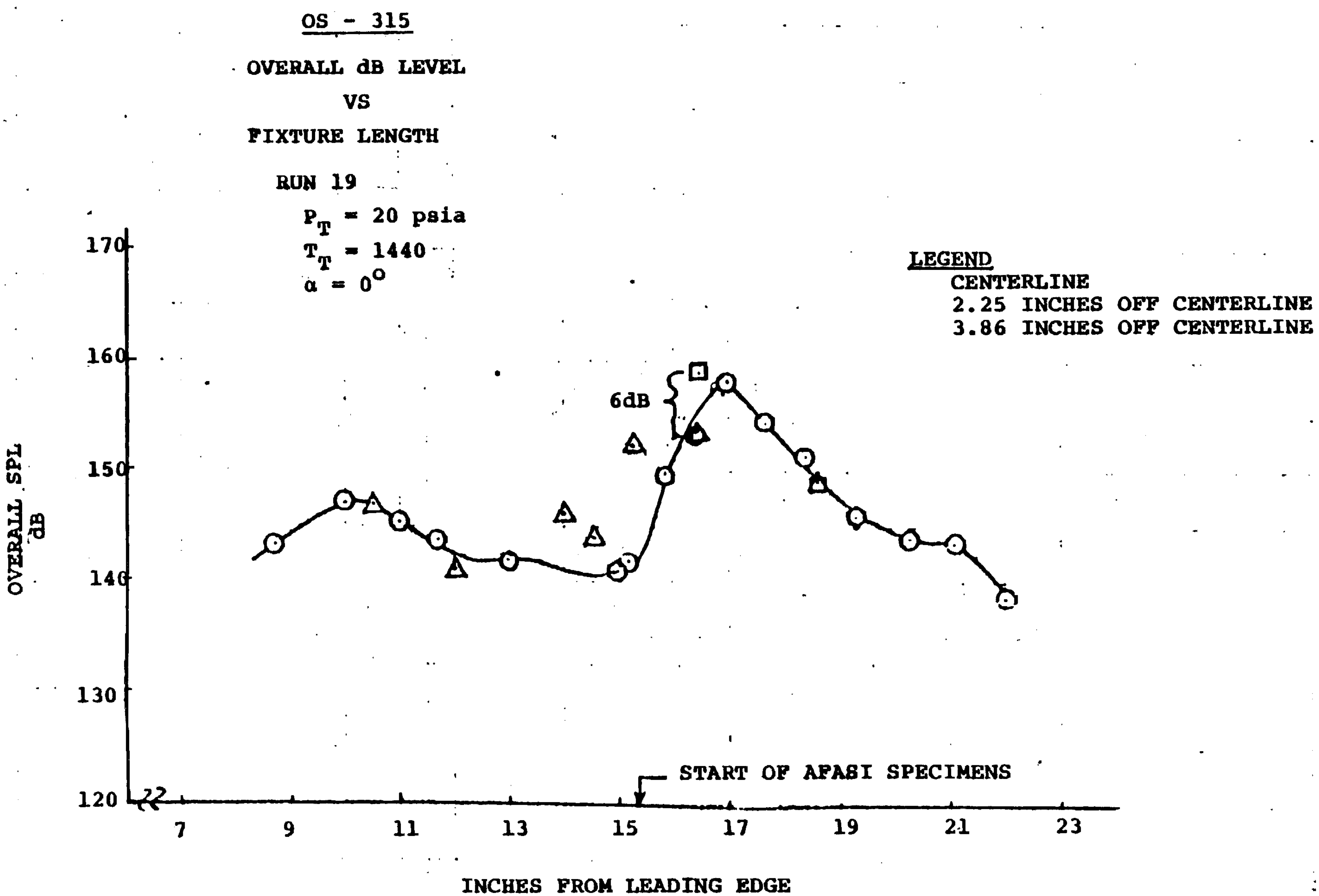

Figure 14.- OASpls on OS-315 fixture for entry simulation, TT=1,440°F.

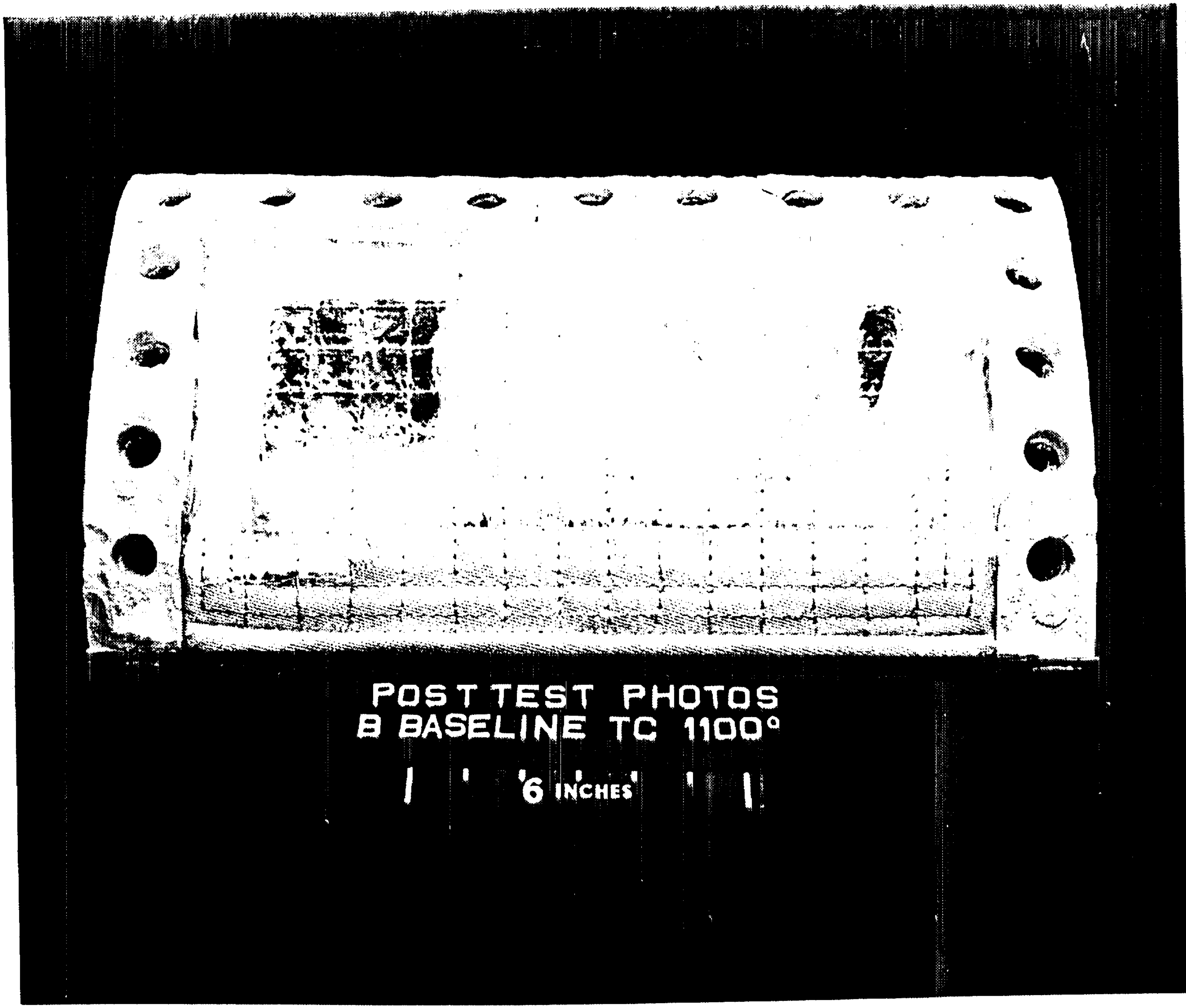

Figure 15. Post test photograph of AFRSI Sample B, 1100°F thermally preconditioned (OS-315).

ORIGINAL PAGE
BLACK AND WHITE PHOTOGRAPH

ORIGINAL PAGE IS
OF POOR QUALITY

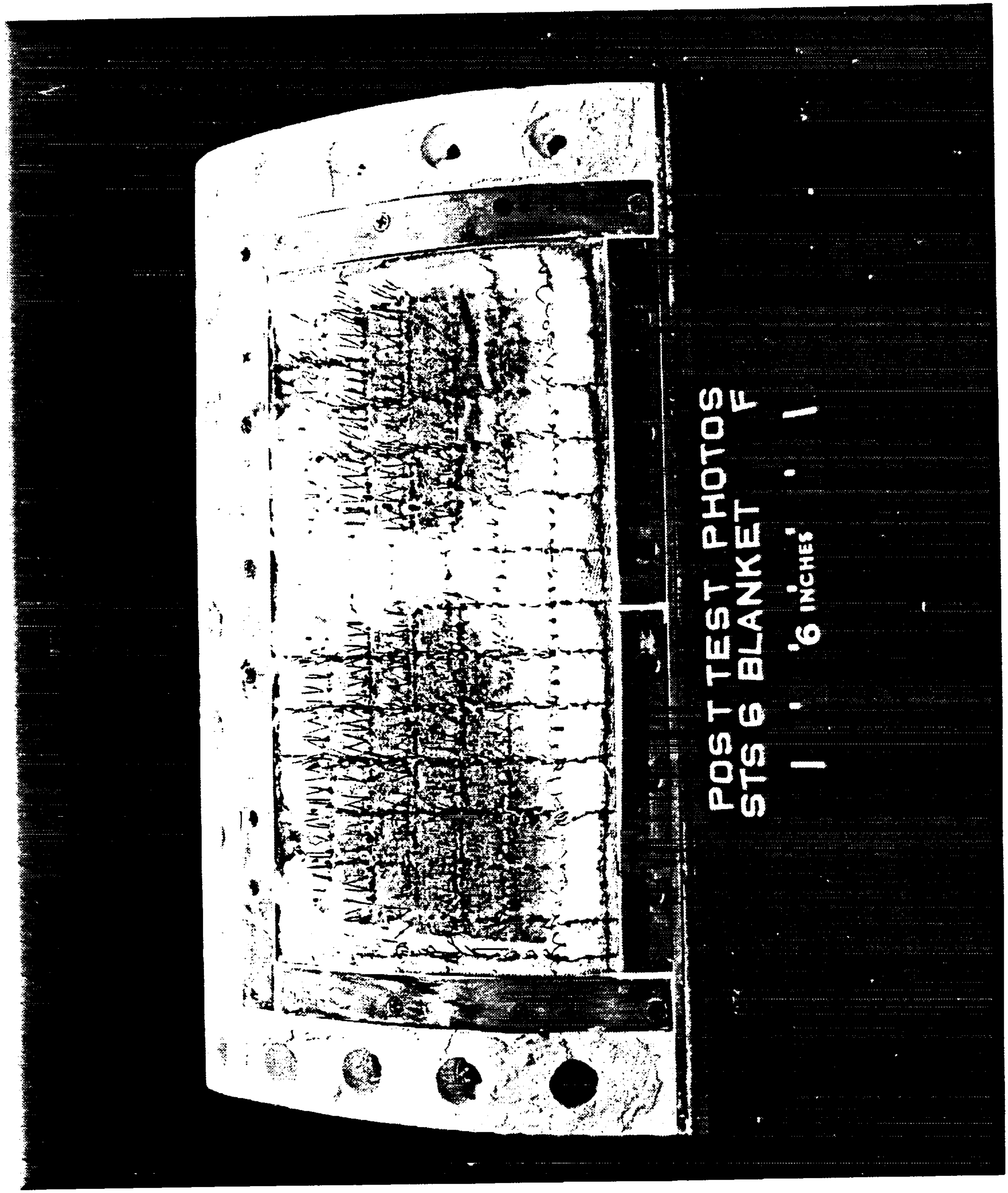

Figure 16.- Post test photograph of AFRSI STS-6 Sample F (OS-315).

ORIGINAL PAGE
BLACK AND WHITE PHOTOGRAPH

ORIGINAL PAGE IS
OF POOR QUALITY

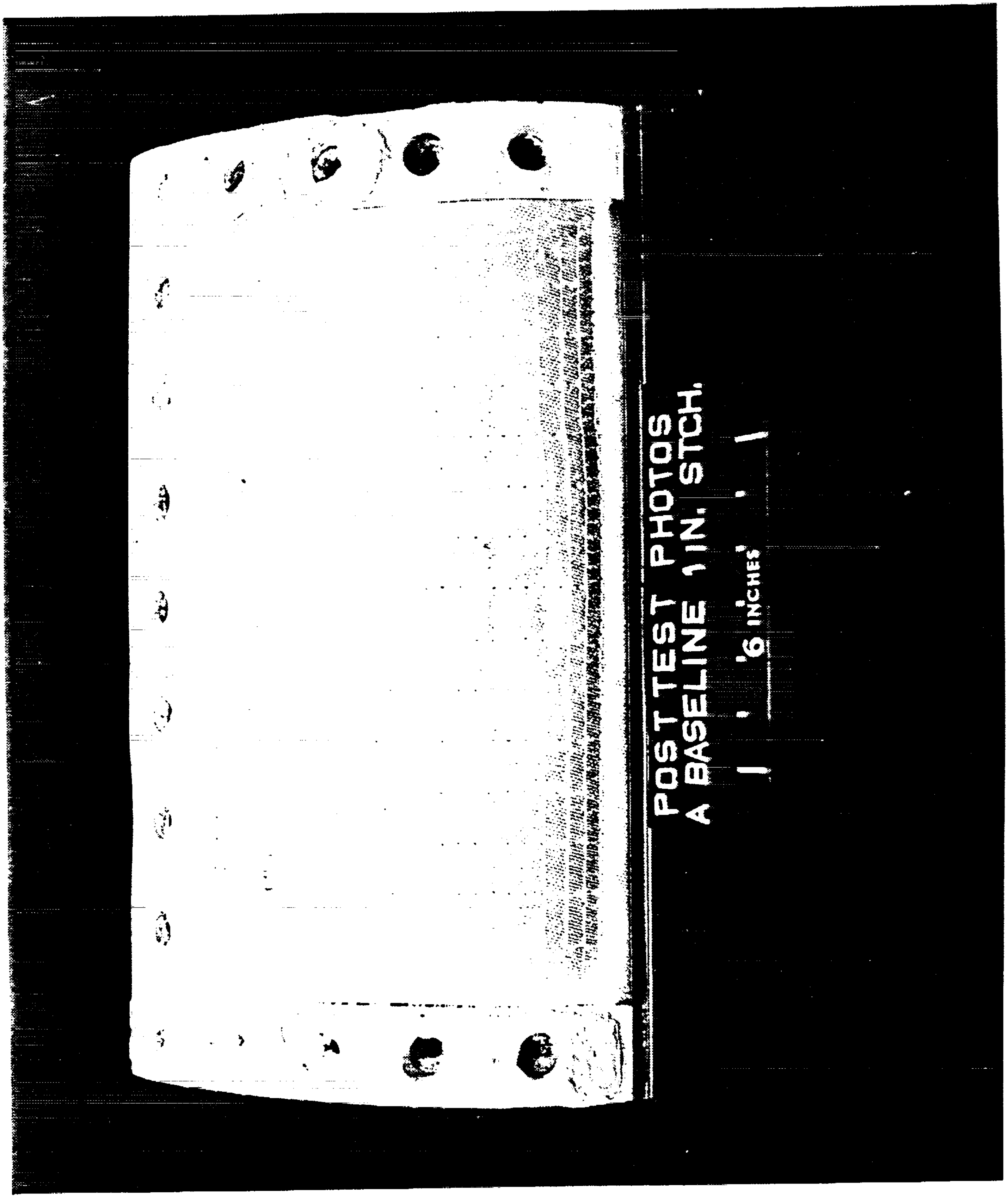

Figure 17.- Post photograph of AFRSI baseline Sample A (OS-315).

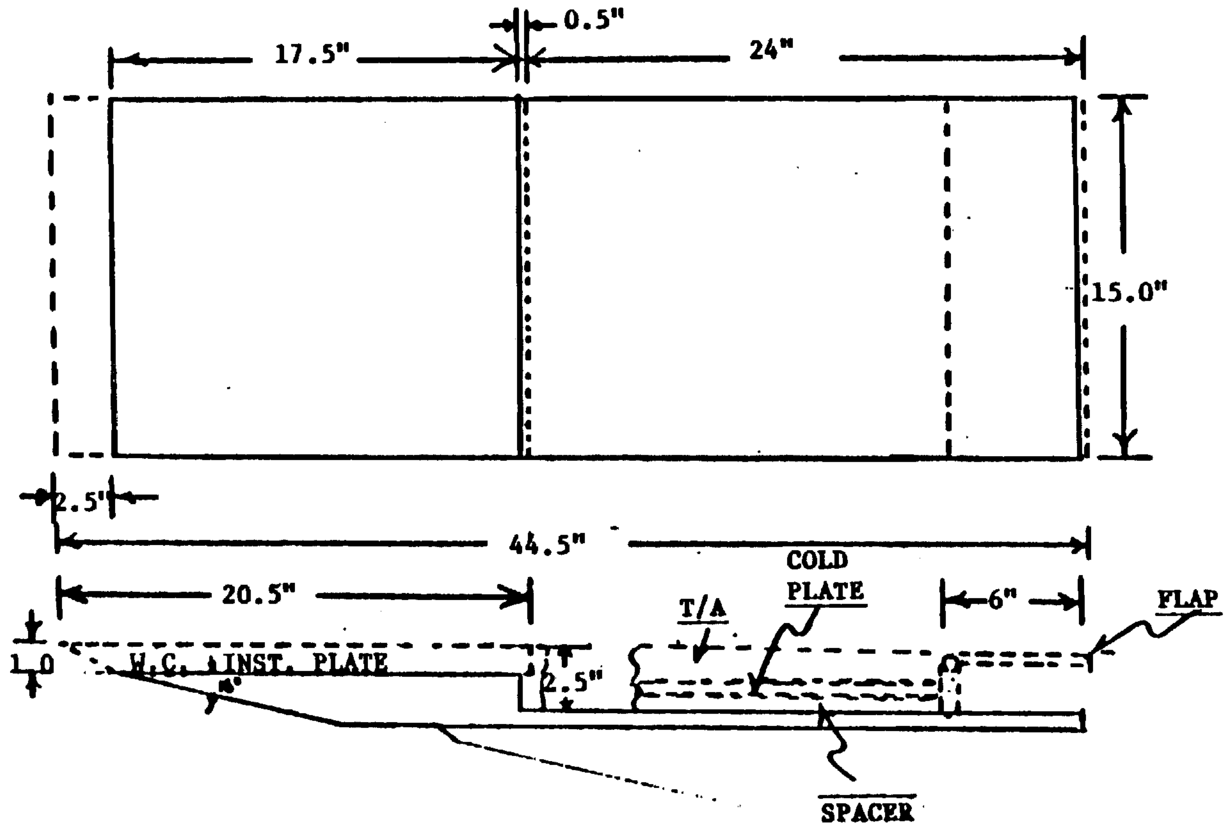

FIGURE 18. MODEL 130-Ø TEST FIXTURE SCHEMATIC
(AEDC WEDGE PLATE MODIFIED)

ORIGINAL PAGE IS
OF POOR QUALITY

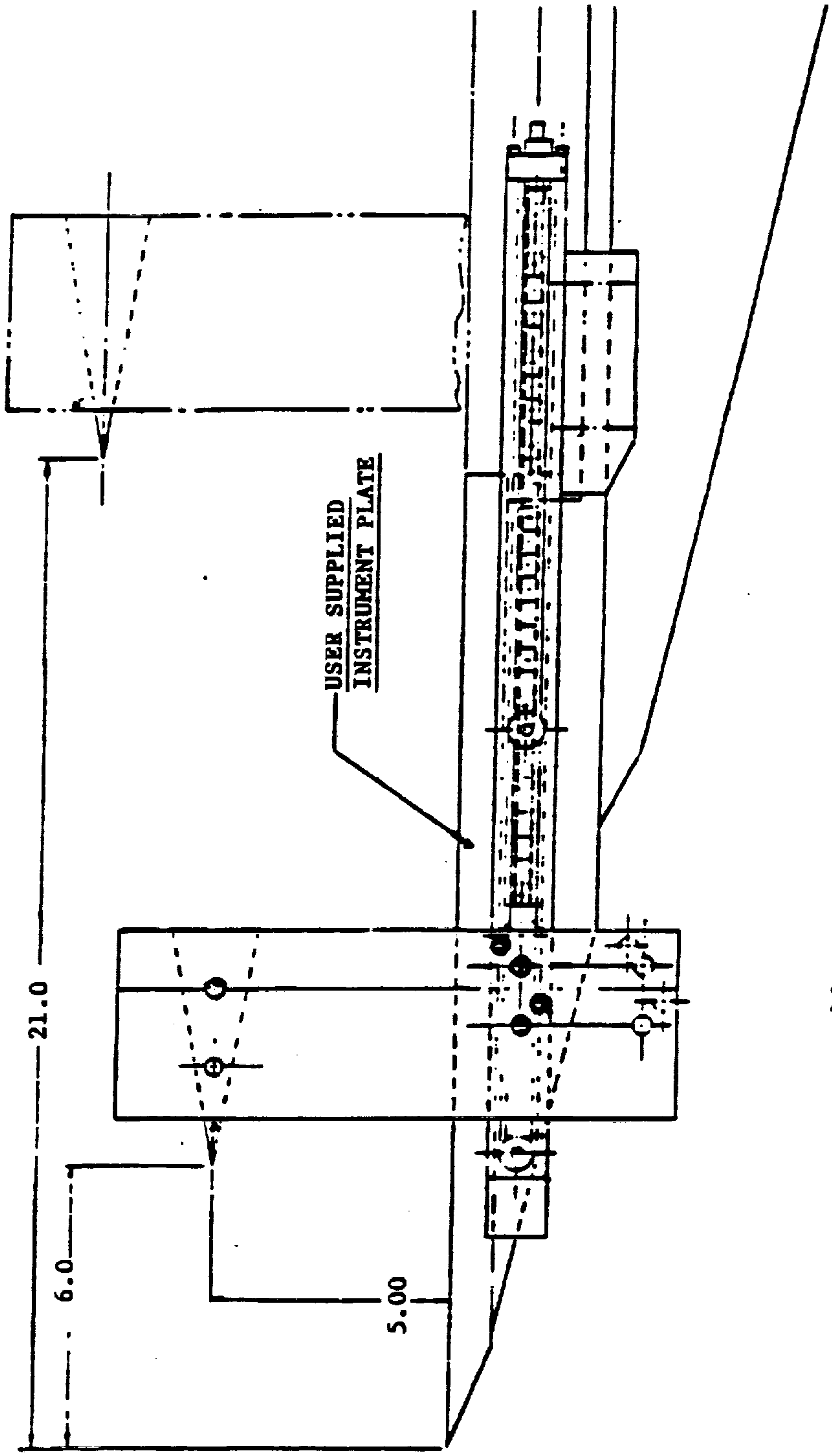

FIGURE 19. SHOCK GENERATOR ASSEMBLY

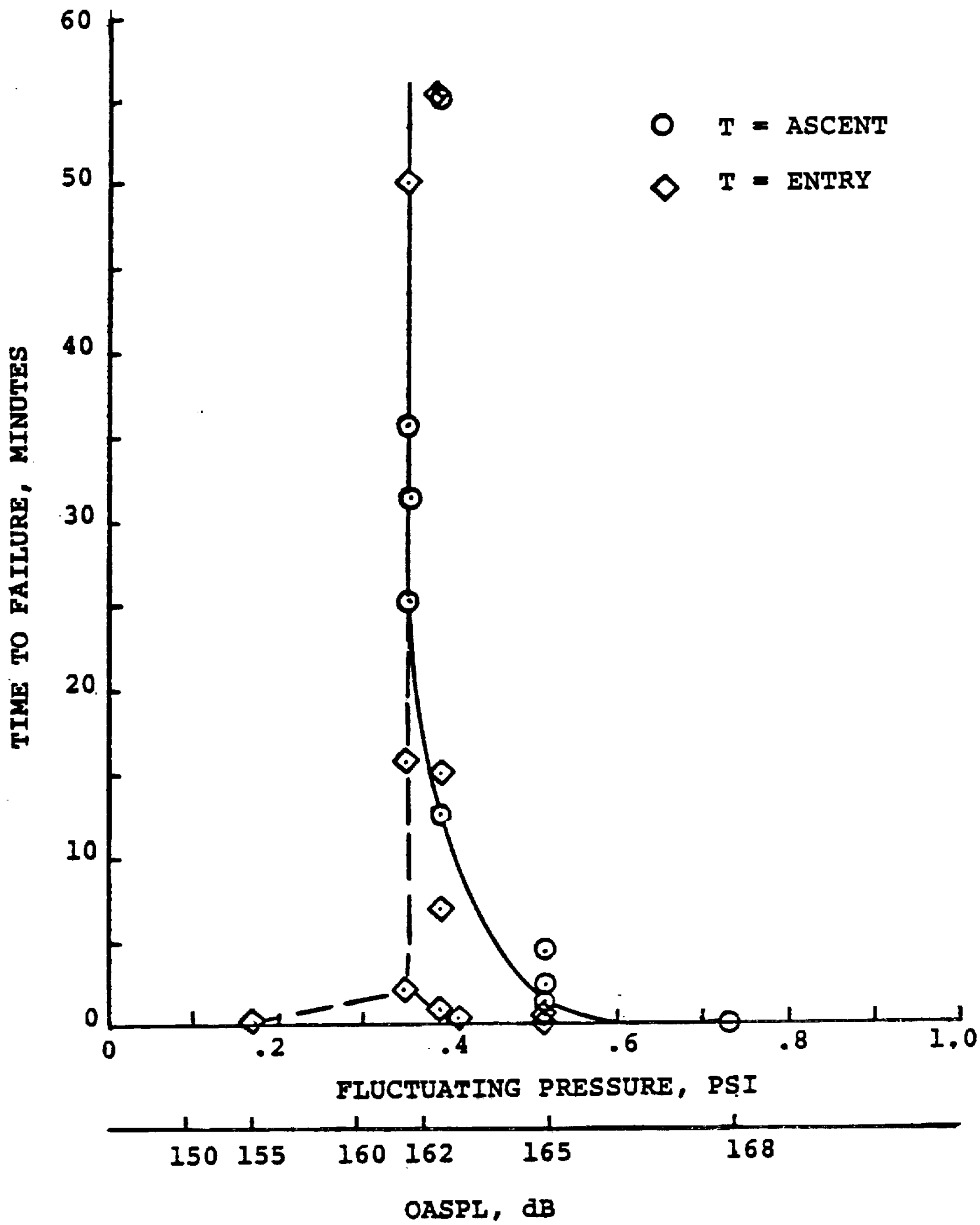

Figure 20.- Time to failure baseline AFRSI tested during OS-318.

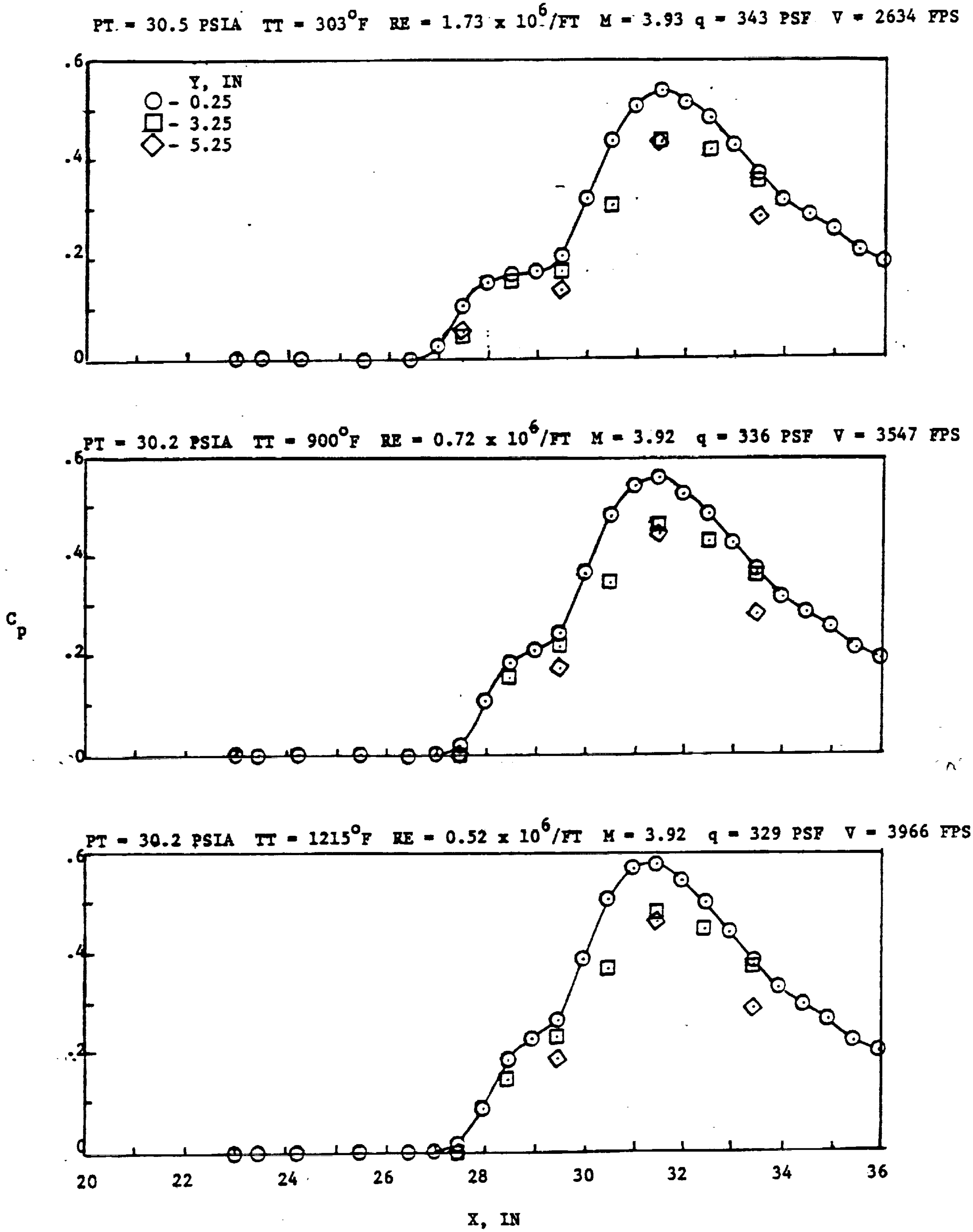

Figure 21.- Surface pressures on the OS-318 test fixture with the 21° wedge shock generator at X=18 inches.

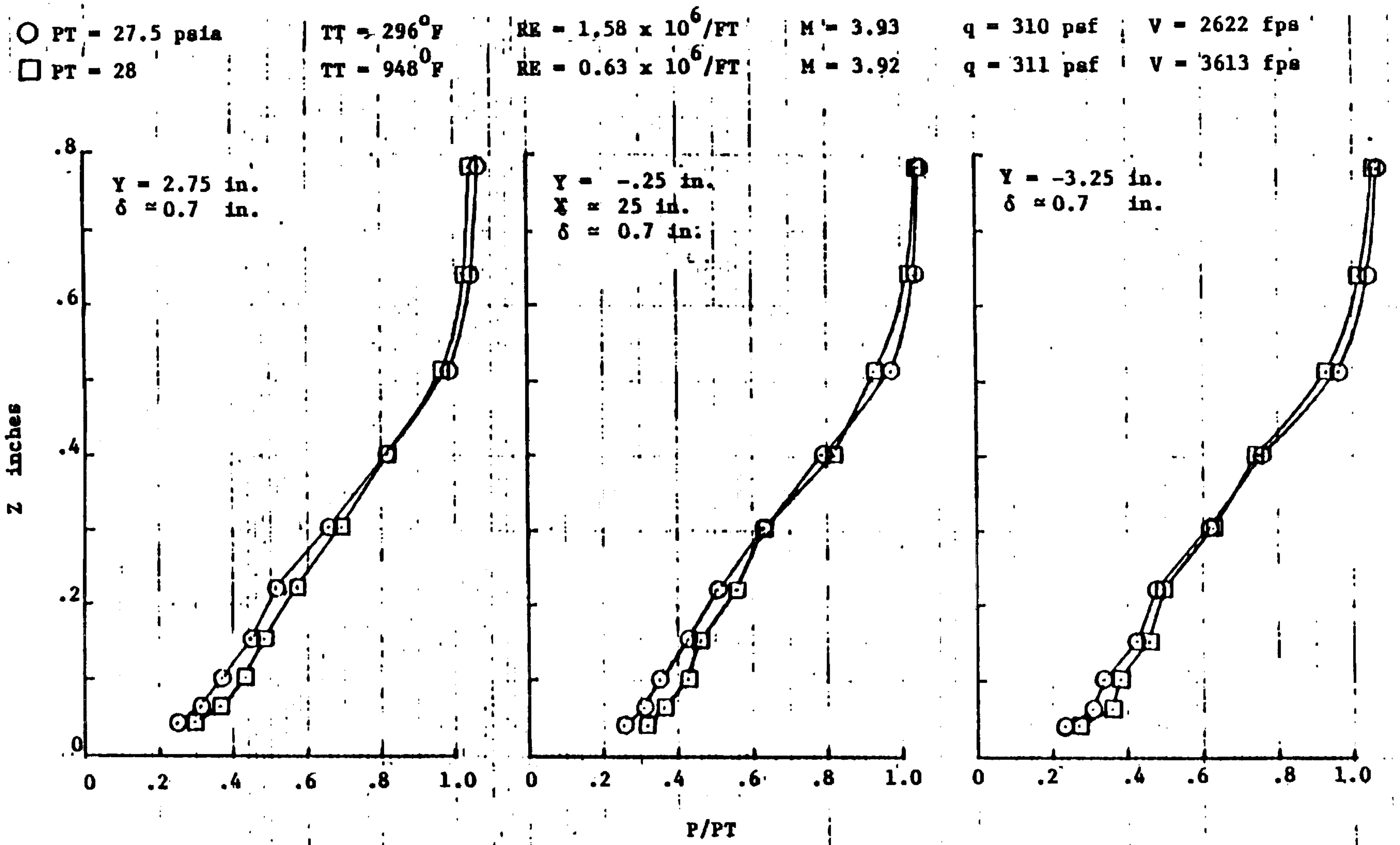

Figure 22.- Boundary-layer profiles on the OS-318 test fixture.

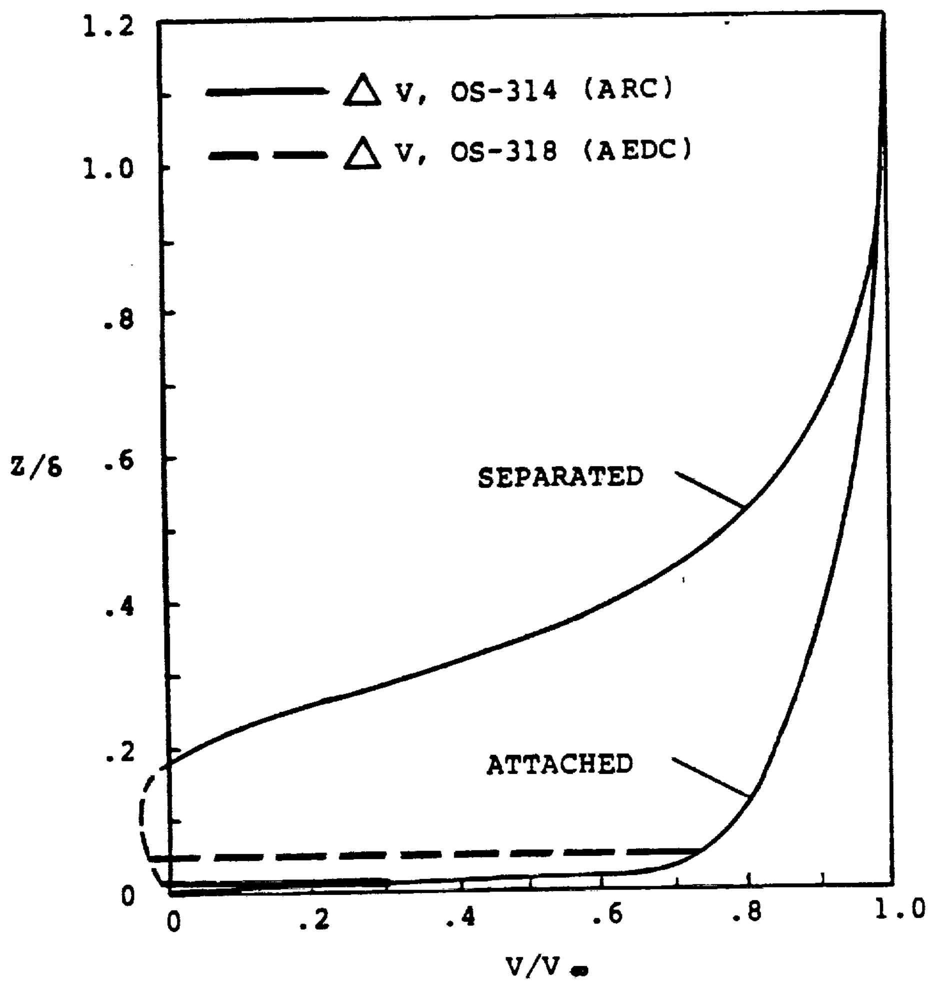

Figure 23.- Illustration of the source of pulsating drag loads on AFRSI quilt stitching.

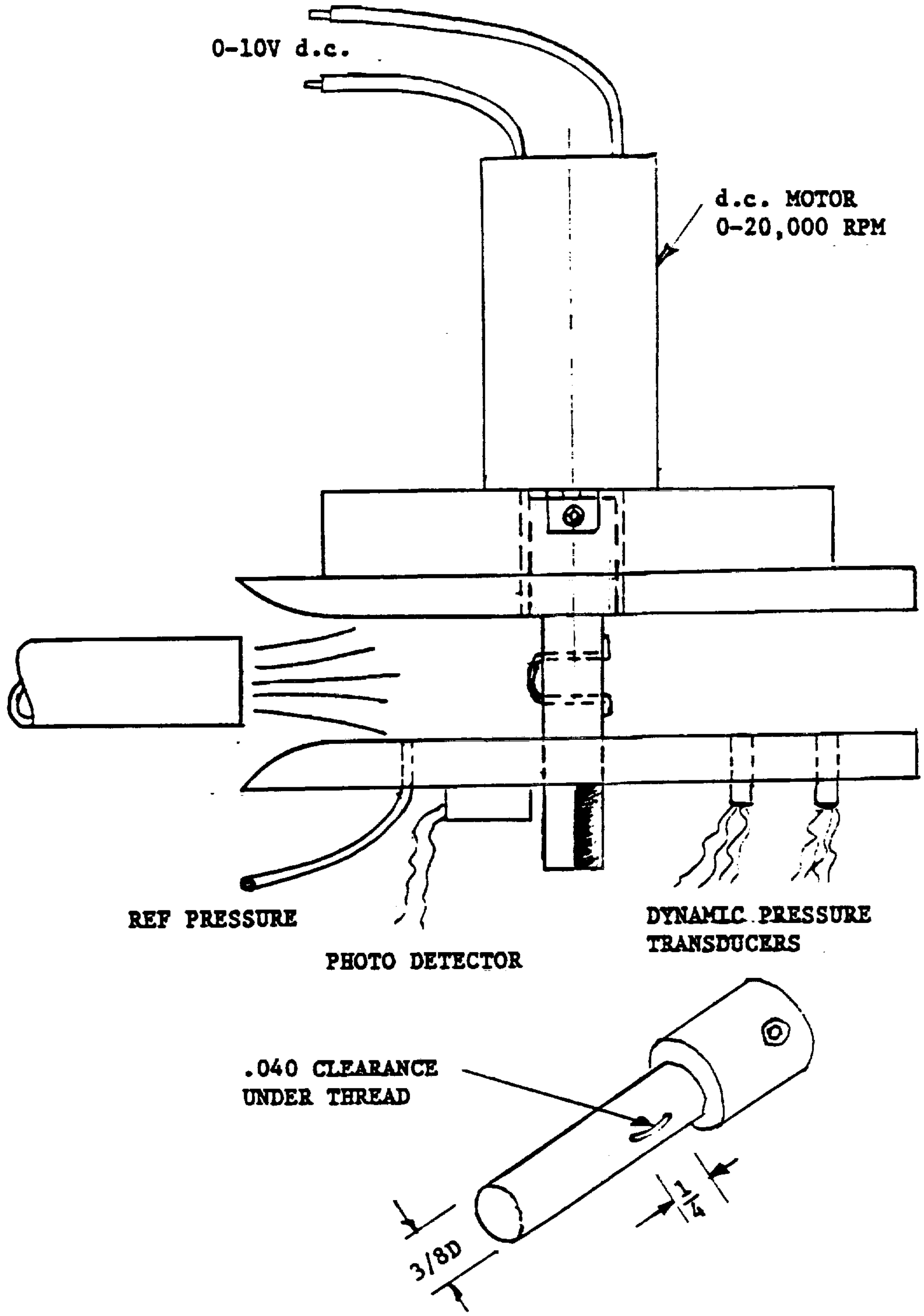

Figure 24.- AFRSI thread test apparatus.

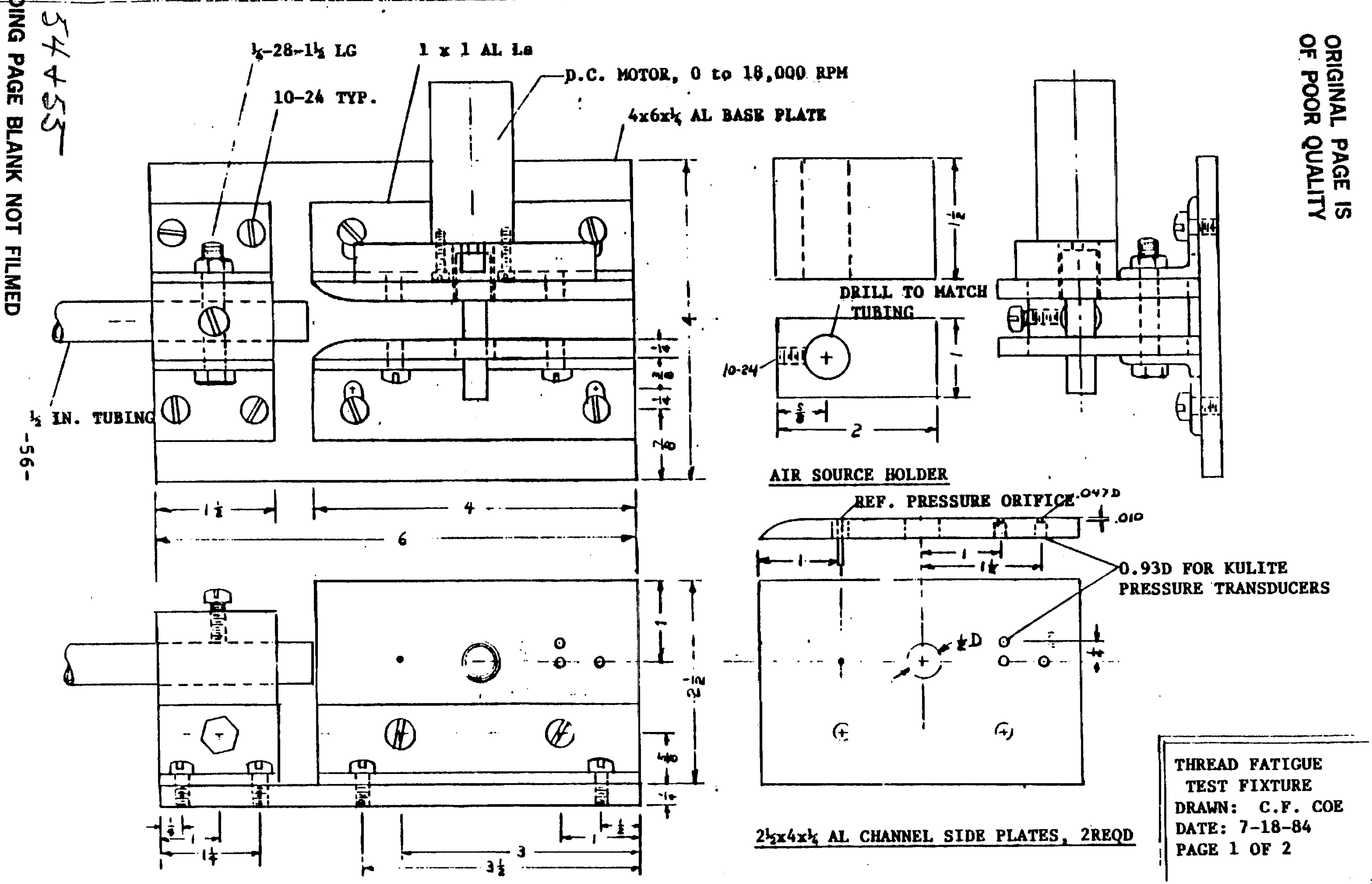

(a) Assembly

Figure 26.- Details of the AFRSI thread fatigue test apparatus.

54+55

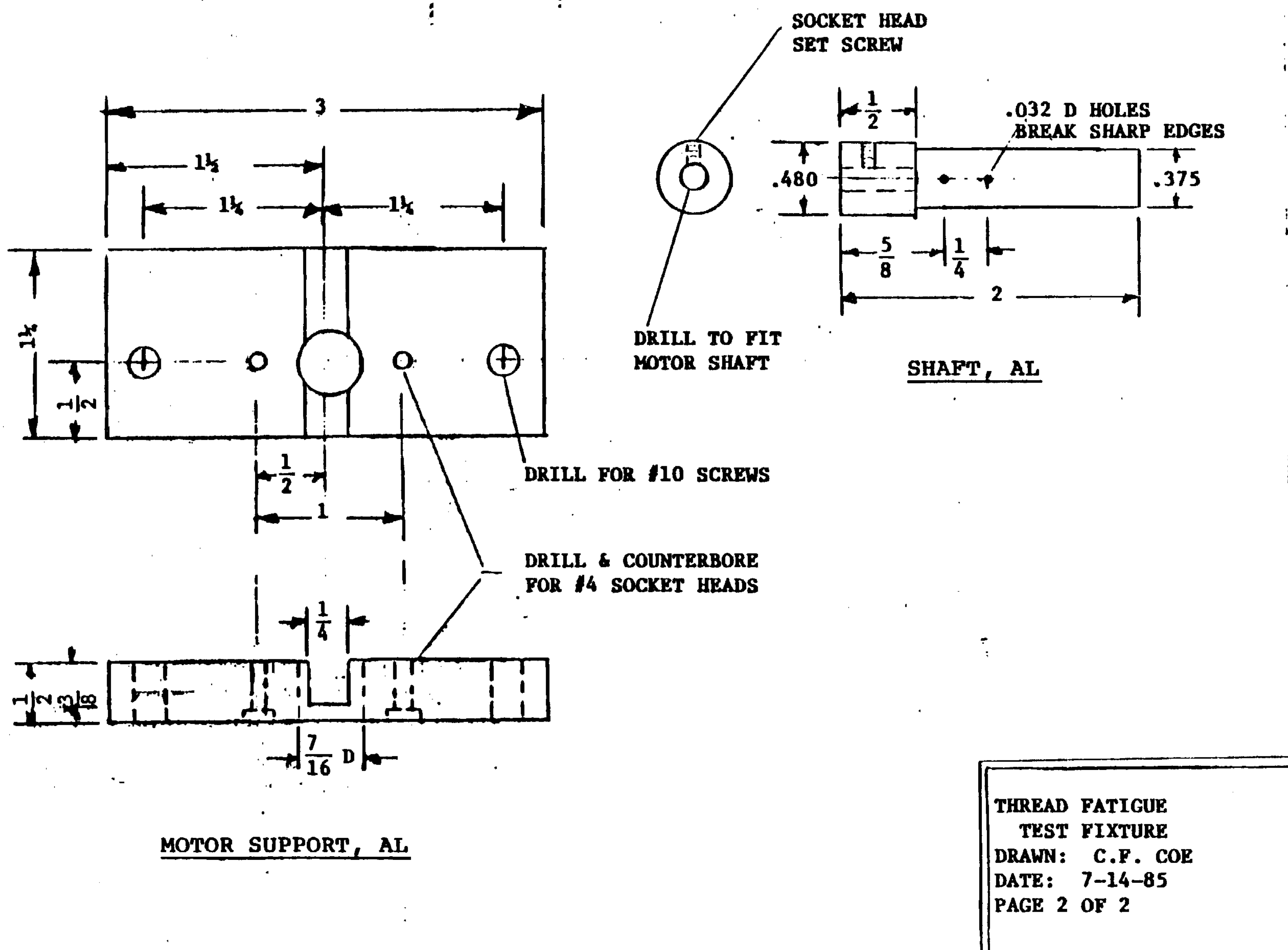

(b) Motor support and shaft
Figure 26.- Concluded.

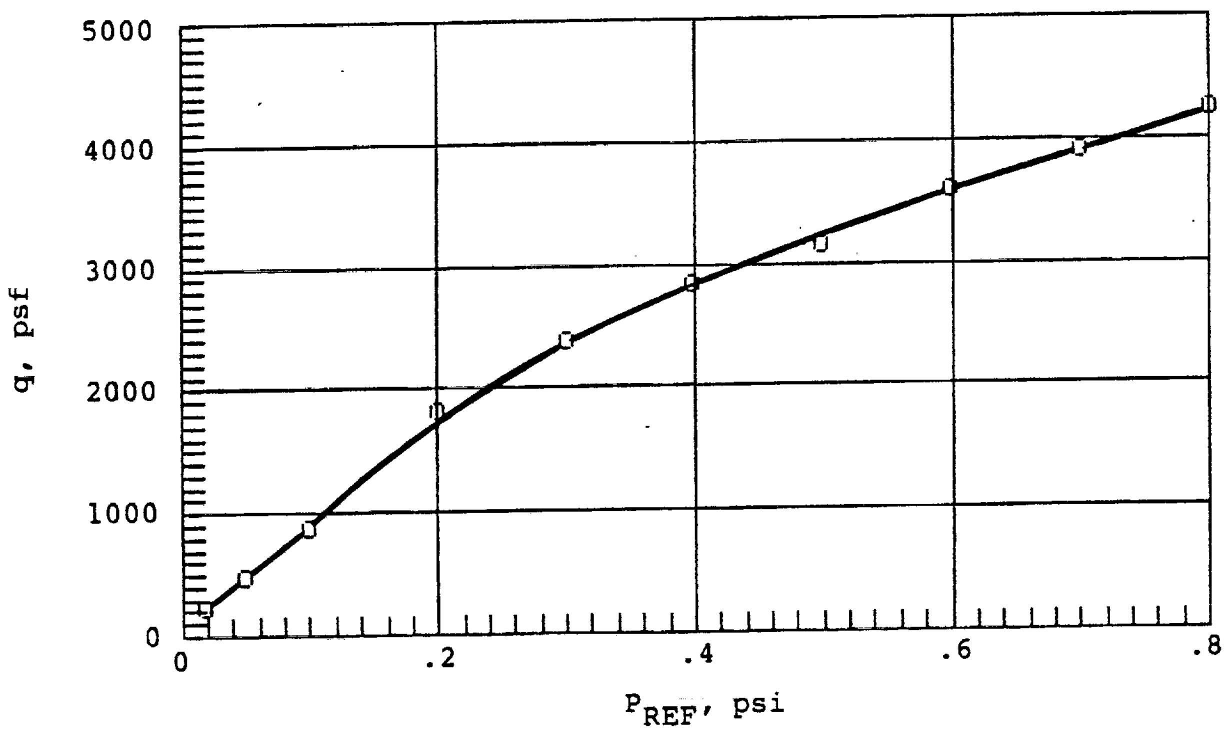

Figure 27.- Dynamic pressure in AFRSI thread test channel versus reference pressure.

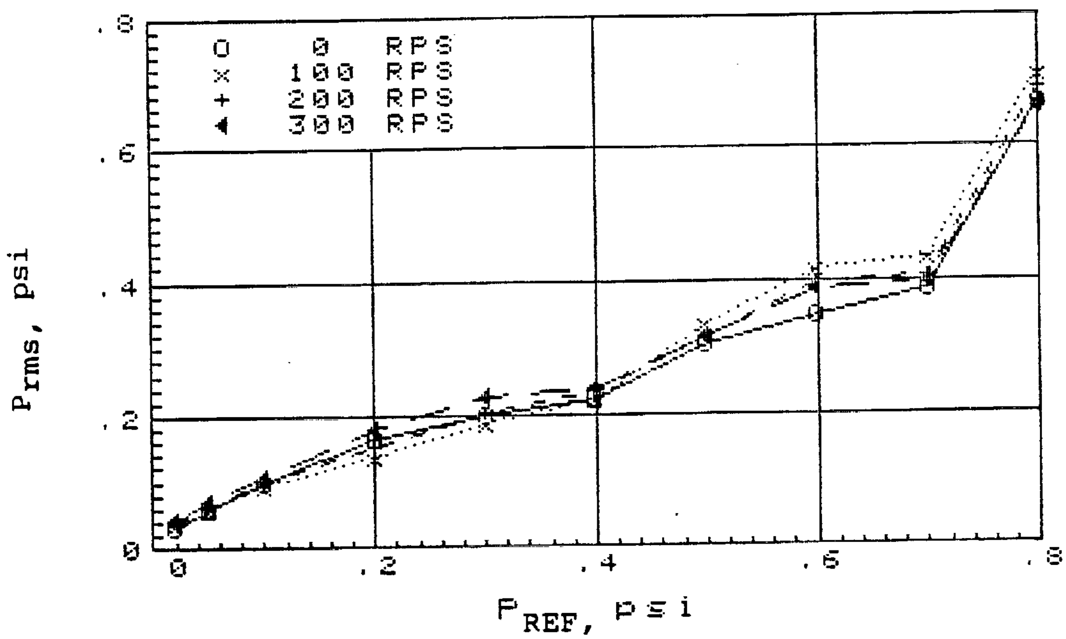

(a) Pressure fluctuations

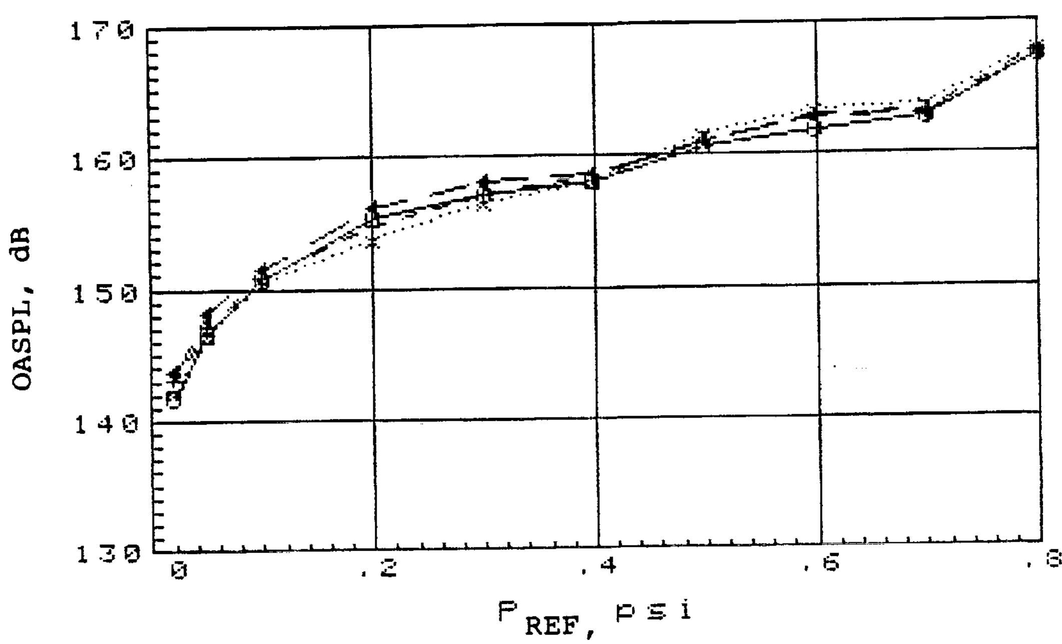

(b) Overall sound pressure levels

Figure 28.- Pressure fluctuations on wall 1-inch downstream of shaft centerline.

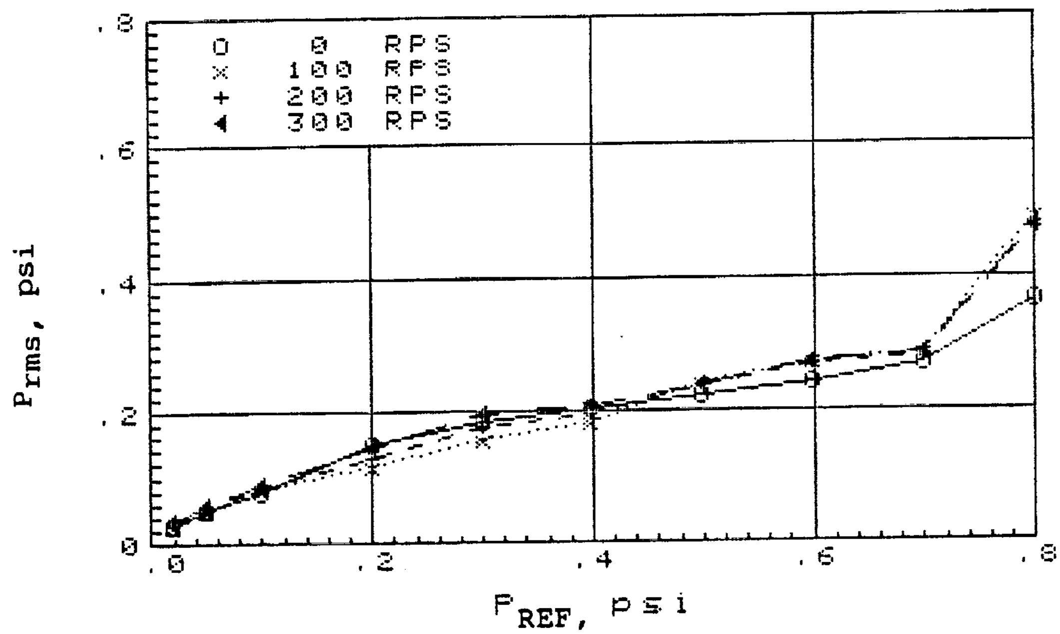

(a) Pressure fluctuations

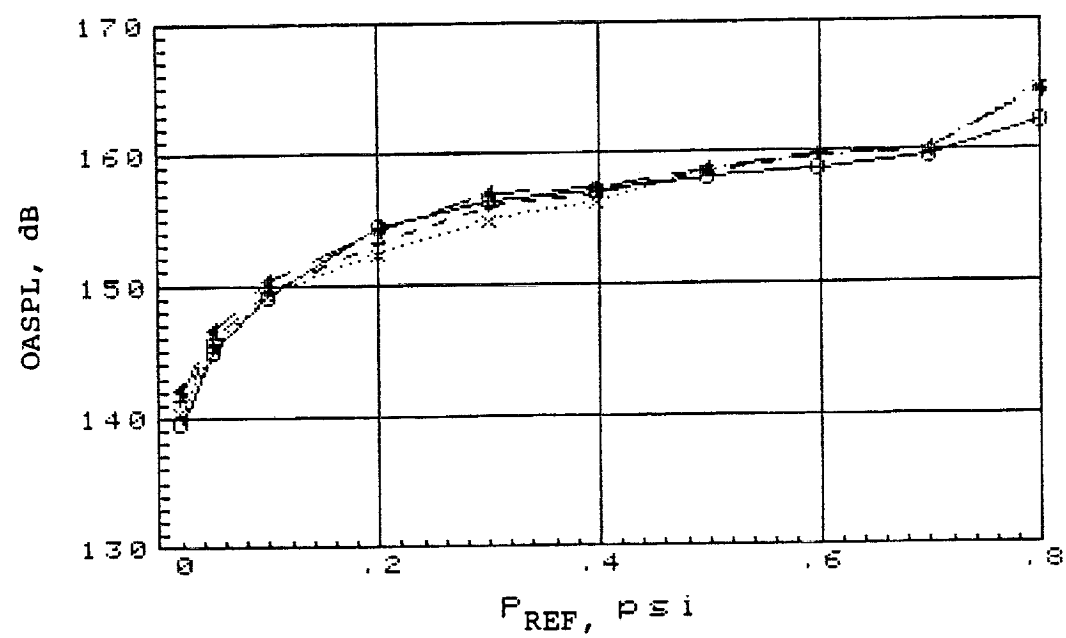

(b) Overall sound pressure levels

Figure 29.- Pressure fluctuations on wall 1 1/2-inch downstream of shaft centerline.

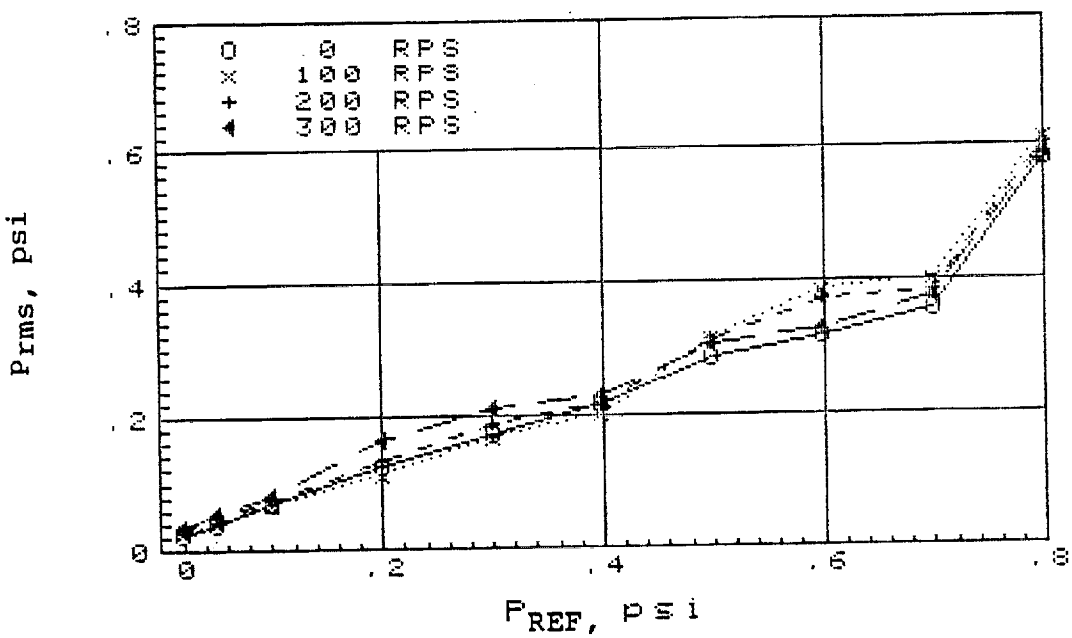

(a) Pressure fluctuations

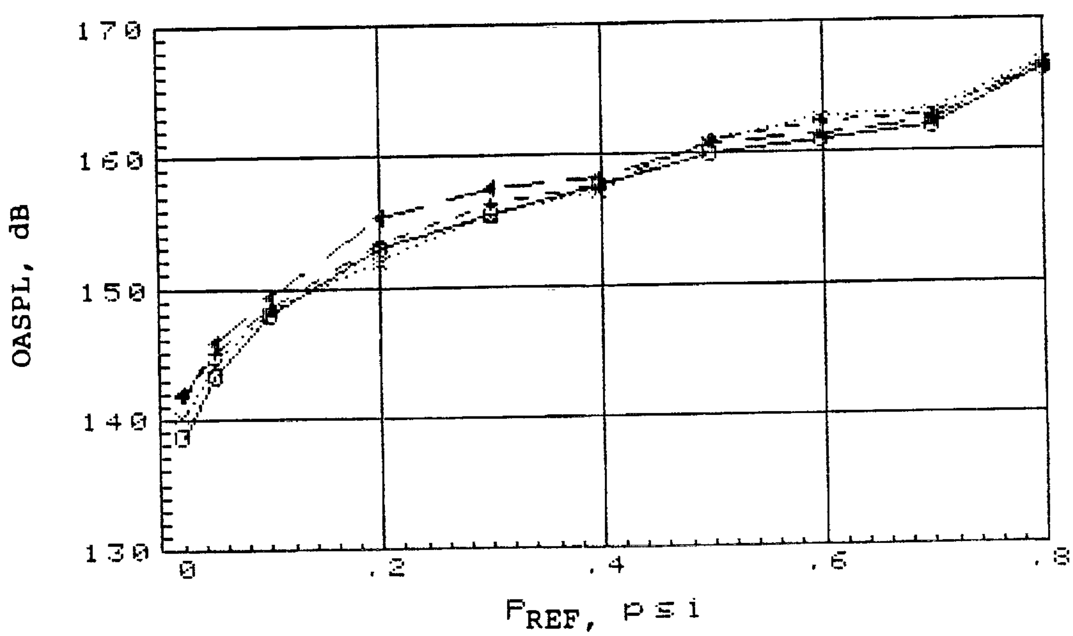

(b) Overall sound pressure levels

Figure 30.- Pressure fluctuations on wall 1-downstream and 1/4-inch above shaft centerline.

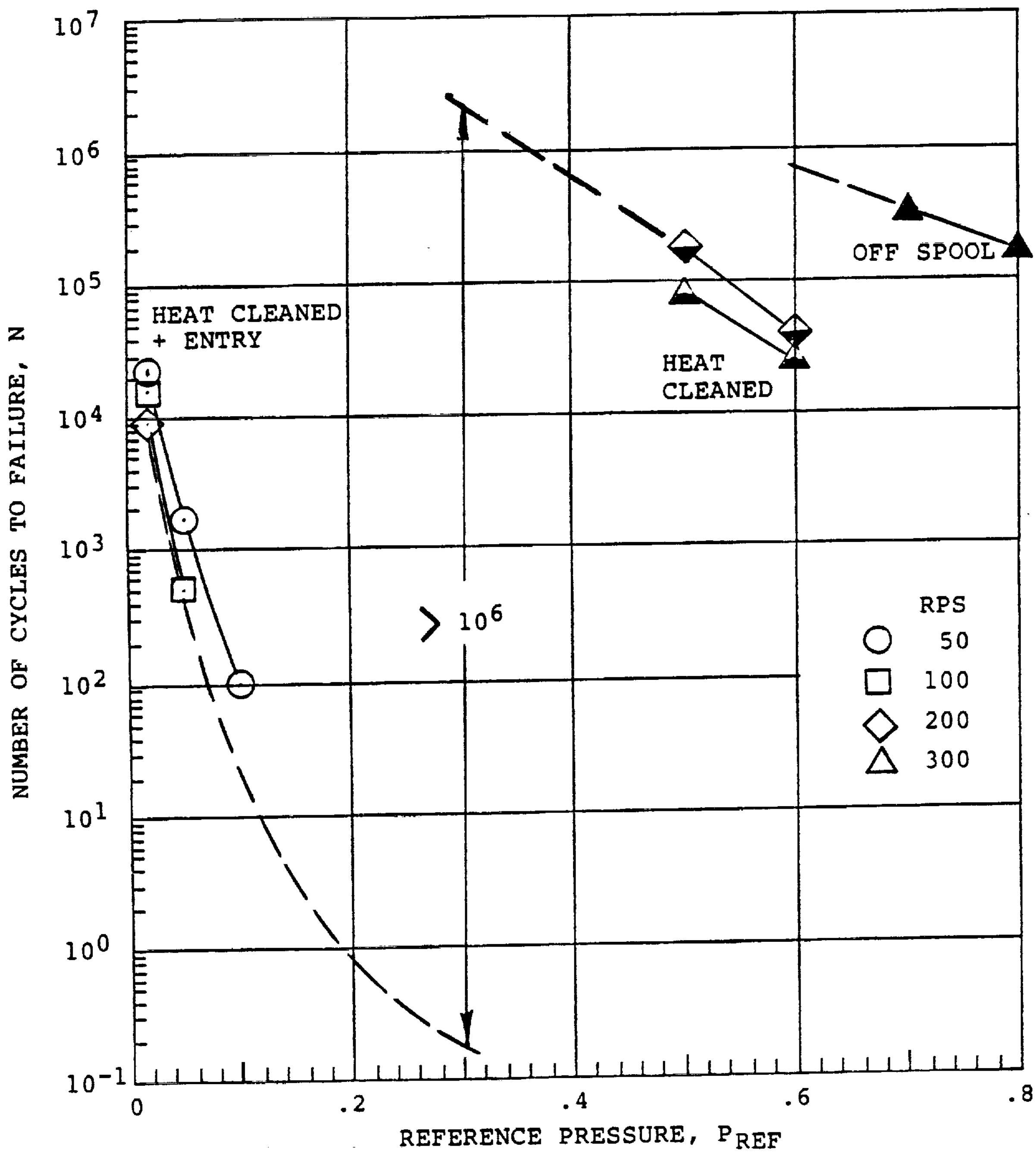

Figure 31.- Number of cycles to failure of AFRSI threads versus reference pressure.

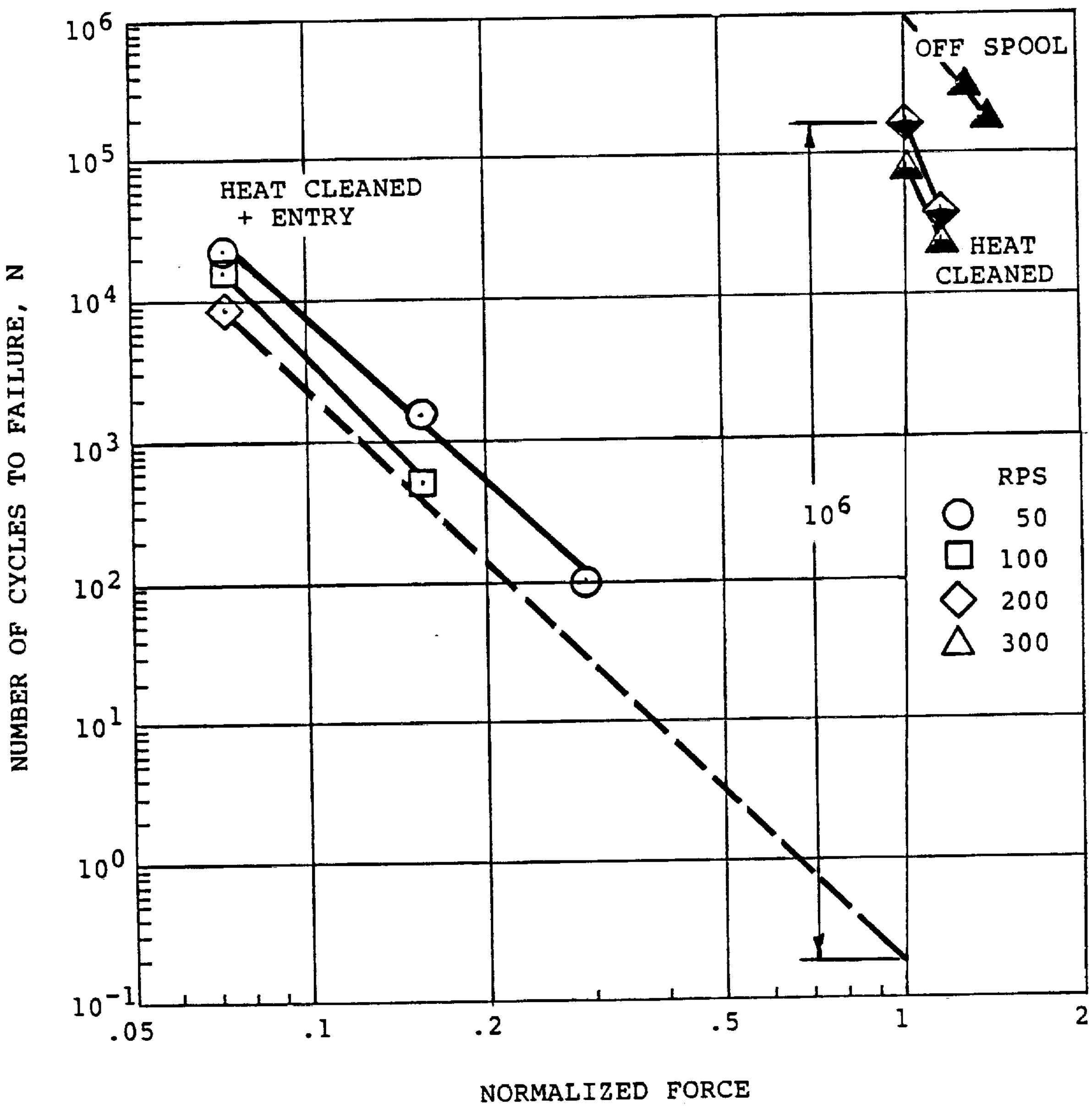

Figure 32.- Number of cycles to failure of AFRSI threads versus normalized force.

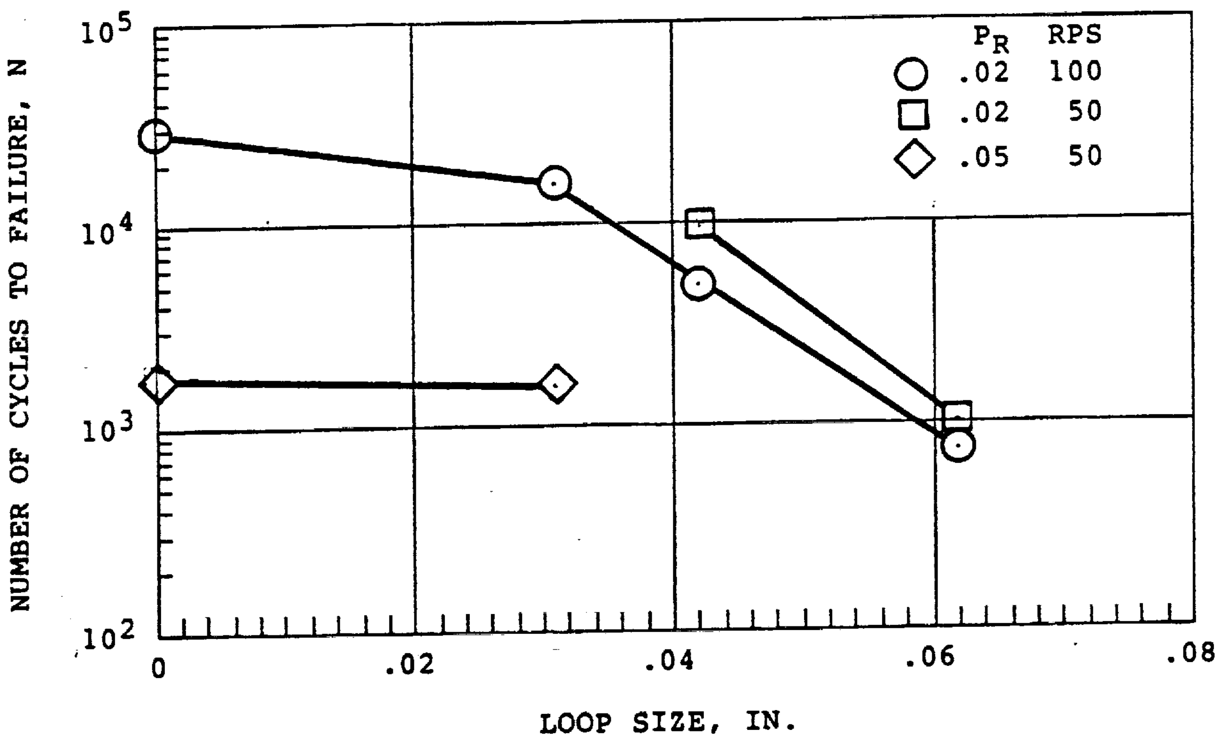

Figure 34.- Effects of loop clearance on number of cycles to failure of AFRSI entry preconditioned thread.

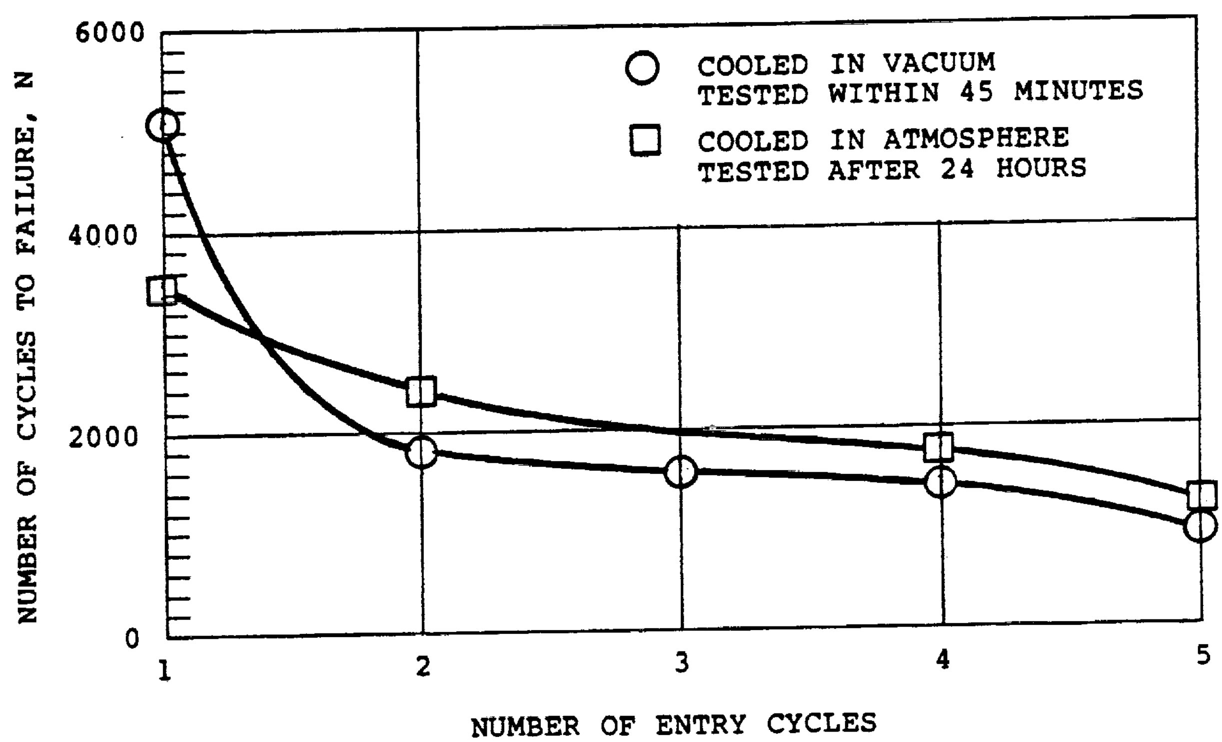

64465

Figure 35.- Effects of number of entry thermal preconditioning cycles in vacuum and air on cycles to failure of AFRSI thread.

PRECEDING PAGE BLANK NOT FILMED

NASA
National Aeronautics and Space Administration

Report Documentation Page

1. Report No. NASA CR177466	2. Government Accession No.	3. Recipient's Catalog No.
4. Title and Subtitle An Assessment of Wind Tunnel Test Data on Flexible Thermal Protection Materials and Results of New Fatigue Tests of Threads		5. Report Date April 1985
		6. Performing Organization Code
7. Author(s) Charles Coe, Coe Engineering, Mountain View. CA		8. Performing Organization Report No.
		10. Work Unit No. 506-43-31
9. Performing Organization Name and Address NASA Ames Research Center, Moffett Field, CA 94035		11. Contract or Grant No. NAS2-11420
		13. Type of Report and Period Covered Contractor Report
12. Sponsoring Agency Name and Address National Aeronautics and Space Administration, Washington, DC 20546		14. Sponsoring Agency Code

15. Supplementary Notes
Point of Contact: S.R. Riccitiello, Ames Research Center, MS 234-1, Moffett Field, CA 94035 - (415) 694-6080 or FTS 464-6080.

16. Abstract
Advanced Flexible Reusable Surface Insulation (AFRSI) has been developed as a replacement for the low-temperature (white) tiles on the Space Shuttle. The first use of the AFRSI for an Orbiter flight was on the OMS POD of Orbiter .099 for STS-6. Post flight examination after STS-6 showed that damage had occurred to the AFRSI during flight. The failure anomaly between previous wind-tunnel test and STS-6 prompted a series of additional wind-tunnel tests to gain an insight as to the cause of the failure. An assessment of all the past STS- wind tunnel tests pointed out the sensitivity of the test results to scaling of dynamic loads due to the difference of boundary layer thickness, and the material properties as a result of exposure to heating.

The thread component of the AFRSI was exposed to fatigue testing using an apparatus that applied pulsating aerodynamic loads on the threads similar to the loads caused by an oscillating shock. Comparison of the mean values of the number-of-cycles to failure showed that the history of the thread was a major factor in its performance. The thread and the wind tunnel data suggests a mechanism of failure for the AFRSI.

17. Key Words (Suggested by Author(s)) Flexible TPS, Flexible TPS Component Testing, Assessment of AFRSI Wind Tunnel Tests		18. Distribution Statement [redacted] Subject Category: 71	
19. Security Classif. (of this report) Unclass.	20. Security Classif. (of this page) Unclass.	21. No. of pages 27	22. Price A03

NASA FORM 1626 OCT 86

PREPARATION OF THE REPORT DOCUMENTATION PAGE

The last page of a report facing the third cover is the Report Documentation Page, RDP. Information presented on this page is used in announcing and cataloging reports as well as preparing the cover and title page. Thus it is important that the information be correct. Instructions for filling in each block of the form are as follows:

Block 1. Report No. NASA report series number, if preassigned.

Block 2. Government Accession No. Leave blank.

Block 3. Recipient's Catalog No. Reserved for use by each report recipient.

Block 4. Title and Subtitle. Typed in caps and lower case with dash or period separating subtitle from title.

Block 5. Report Date. Approximate month and year the report will be published.

Block 6. Performing Organization Code. Leave blank.

Block 7. Author(s). Provide full names exactly as they are to appear on the title page. If applicable, the word editor should follow a name.

Block 8. Performing Organization Report No. NASA installation report control number and, if desired, the non-NASA performing organization report control number.

Block 9. Performing Organization Name and Address. Provide affiliation (NASA program office, NASA installation, or contractor name) of authors.

Block 10. Work Unit No. Provide Research and Technology Objectives and Plans (RTOP) number.

Block 11. Contract or Grant No. Provide when applicable.

Block 12. Sponsoring Agency Name and Address. National Aeronautics and Space Administration, Washington, D.C. 20546-0001. If contractor report, add NASA installation or HQ program office.

Block 13. Type of Report and Period Covered. NASA formal report series; for Contractor Report also list type (interim, final) and period covered when applicable.

Block 14. Sponsoring Agency Code. Leave blank.

Block 15. Supplementary Notes. Information not included elsewhere: affiliation of authors if additional space is required for block 9, notice of work sponsored by another agency, monitor of contract, information about supplements (film, data tapes, etc.), meeting site and date for presented papers, journal to which an article has been submitted, note of a report made from a thesis, appendix by author other than shown in block 7.

Block 16. Abstract. The abstract should be informative rather than descriptive and should state the objectives of the investigation, the methods employed (e.g., simulation, experiment, or remote sensing), the results obtained, and the conclusions reached.

Block 17. Key Words. Identifying words or phrases to be used in cataloging the report.

Block 18. Distribution Statement. Indicate whether report is available to public or not. If not to be controlled, use "Unclassified-Unlimited." If controlled availability is required, list the category approved on the Document Availability Authorization Form (see NHB 2200.2, Form FF427). Also specify subject category (see "Table of Contents" in a current issue of STAR), in which report is to be distributed.

Block 19. Security Classification (of this report). Self-explanatory.

Block 20. Security Classification (of this page). Self-explanatory.

Block 21. No. of Pages. Count front matter pages beginning with iii, text pages including internal blank pages, and the RDP, but not the title page or the back of the title page.

Block 22. Price Code. If block 18 shows "Unclassified-Unlimited," provide the NTIS price code (see "NTIS Price Schedules" in a current issue of STAR) and at the bottom of the form add either "For sale by the National Technical Information Service, Springfield, VA 22161-2171" or "For sale by the Superintendent of Documents, U.S. Government Printing Office, Washington, DC 20402-0001," whichever is appropriate.